NTNU – Trondheim
Norwegian University of
Science and Technology

Process simulation of semi-closed recuperated cycle

Judit Tomás Verde

Master's Thesis
Submission date: March 2015
Supervisor: Lars Olof Nord, EPT

Norwegian University of Science and Technology
Department of Energy and Process Engineering

NTNU

Norwegian University
of Science and Technology

Department of Energy
and Process Engineering

EPT-M-2014-158

MASTER THESIS

for

Student Judit Tomás Verde

Autumn 2014

Process simulation of semi-closed recuperated cycle

Background and objective

In recent years, a power cycle, the semi-closed recuperated cycle (SCRC), has been proposed as an alternative to the widely used combined cycle gas turbine (CCGT) plant. The SCRC technology may have advantages over the CCGT such as an increased power density and being well suited for CO_2 capture. Simplicity and flexibility could be other positives with the technology. An increased power density could make the technology interesting for powering offshore oil and gas installations.

The objectives of the thesis work are to model and simulate an SCRC plant and to compare it with a CCGT plant. A process simulation tool like EBSILON Professional should be used.

The following tasks are to be considered:

1. Literature study related to CCGT, pressurized HRSG, and SCRC.
2. Design and build a process models of a CCGT plant to use as reference plant.
3. Process simulation of the CCGT plant to produce results such as power output, net plant efficiency, and exhaust gas composition.
4. Design and build a process models of an SCRC plant.
5. Process simulation of the SCRC plant to produce results such as power output, net plant efficiency, and exhaust gas composition.
6. Evaluate the results by comparing the different techologies.
7. List some of the challenges with the SCRC technology and propose future work.

Within 14 days of receiving the written text on the master thesis, the candidate shall submit a research plan for his project to the department.

When the thesis is evaluated, emphasis is put on processing of the results, and that they are presented in tabular and/or graphic form in a clear manner, and that they are analyzed carefully.

The thesis should be formulated as a research report with summary, conclusion, literature references, table of contents, etc. During the preparation of the text, the candidate should make an effort to produce a well-structured and easily readable report. In order to ease the evaluation of the thesis, it is important that the cross-references are correct. In the making of the report, strong emphasis should be placed on both a thorough discussion of the results and an orderly presentation.

The candidate is requested to initiate and keep close contact with his/her academic supervisor(s) throughout the working period. The candidate must follow the rules and regulations of NTNU as well as passive directions given by the Department of Energy and Process Engineering.

Risk assessment of the candidate's work shall be carried out according to the department's procedures. The risk assessment must be documented and included as part of the final report. Events related to the candidate's work adversely affecting the health, safety or security, must be documented and included as part of the final report. If the documentation on risk assessment represents a large number of pages, the full version is to be submitted electronically to the supervisor and an excerpt is included in the report.

Pursuant to "Regulations concerning the supplementary provisions to the technology study program/Master of Science" at NTNU §20, the Department reserves the permission to utilize all the results and data for teaching and research purposes as well as in future publications.

The final report is to be submitted digitally in DAIM. An executive summary of the thesis including title, student's name, supervisor's name, year, department name, and NTNU's logo and name, shall be submitted to the department as a separate pdf file. Based on an agreement with the supervisor, the final report and other material and documents may be given to the supervisor in digital format.

☐ Work to be done in lab (Water power lab, Fluids engineering lab, Thermal engineering lab)
☐ Field work

Department of Energy and Process Engineering, 8 September 2014

Olav Bolland
Department Head

Lars Olof Nord
Supervisor

Abstract

Nowadays, the combined cycle gas turbine (CCGT) is the most used technology for electric power generation among the plants that produce electricity from fossil fuels. There are several advantages that made the widespread of this technology. The most important benefits in comparison with conventional thermoelectric plants are a higher efficiency, its flexibility, and acceptable NO_x and CO_2 emissions.

However, in recent years, a power cycle has been suggested as a new choice outperforming the widely used CCGT plants. The most recent proposal is an air breathing semi-closed recuperated cycle (SCRC) which, although it has been proposed since the 1980s, has not been yet practically developed. Such plants have an efficiency potential similar to CCGTs. Flexibility operation, power density, its simplicity, and an increased power density could be advantages over the CCGT plants as well as being well suited for CO_2 capture. Furthermore, a SCRC does not require any inexistent technology that has not been proved before in large CCGTs or gas turbine plants (GT).

Hence, a comparison between a CCGT plant and the innovative SCRC technology has been developed in this project. For achieving this objective, a SCRC was designed on the basis of recent studies, and a CCGT was based on theory and operating plants. The simulations of these models were carried out using EBSILON®Professional. After comparing both thermodynamic cycles and seeing the advantages and inconveniences of the semi-closed cycle studied, a sensitivity analysis of the SCRC was developed in order to know how determined changes in the design point influenced on the plant. To conclude this project, the most relevant aspects regarding potential, future work, and challenges with the SCRC technology were listed.

Preface

This thesis, *Process simulation of semi-closed recuperated cycle*, has been written as a Master Thesis of Judit Tomás Verde. The final work is the result of a 5-year studies of Chemical Engineering at the Universitat Politècnica de Catalunya (UPC). The thesis has been written in Trondheim, for the Department of Energy and Process Engineering at the Norwegian University of Science and Technology (NTNU).

The main aim of the work is to determine the advantages and inconveniences of a semi-closed recuperated cycle compared to a combined cycle gas turbine by simulating both cycles.

Last but not least, I would like to thank my supervisor Lars O. Nord for his help and advice throughout these months of work.

March 16th 2015, Trondheim

Judit Tomás Verde

Table of contents

Figure List

Table list

Abbreviations and acronyms

CCGT	Combined cycle gas turbine
CCS	Carbon capture and storage
DCSG	Direct contact steam generator
EGR	Exhaust gas recirculation
G	Generator
GT	Gas turbine
HP	High pressure
HiPrOx	High pressure oxy-fired
HPRTE	High pressure regenerative turbine engine
HRSG	Heat recovery steam generator
ISO	International Organization for Standardization
LP	Low pressure
NG	Natural gas
PoWER	Power, water extraction and refrigeration
SAGD	Steam assisted gravity drainage
SCRC	Air breathing semi-closed recuperated cycle
ST	Steam turbine
TIT	Turbine inlet temperature

Chemical symbols

Ar	Argon
CO_2	Carbon dioxide
CO	Carbon monoxide
CH_4	Methane
N_2	Nitrogen
NO_x	Nitrogen oxides
O_2	Oxygen
SO_2	Sulfur dioxide
H_2O	Water/steam
UHC	Unburned hydrocarbons

Nomenclature[1]

$\dot{m}_{air}$	Mass flow rate of air	[kg/s]
$\dot{m}_{cw}$	Mass flow rate of cooling water	[kg/s]
$\dot{m}_{fuel}$	Mass flow rate of fuel	[kg/s]
$\dot{m}_{out,GT}$	Mass flow rate after gas turbine	[kg/s]
Q_i	Heat power exchanged in *i*	[kW]
$W_{net,plant}$	Plant net power	[kW]
X_{CO_2}	CO_2 mass concentration in exhaust gas	[kg_{CO2}/kg]
ΔT	Temperature difference	[K]
CO2R	Specific CO_2 flow rate	[kg/kWh]
C_P	Specific heat capacity of water	[kJ/(kgK)]
LHV	Lower heating value	[kJ/kg]
RR	Recirculation ratio	[-]
s	Specific entropy	[kJ/(kgK)]
SP	Specific power	[kJ/kg_{air}]
T	Temperature	[ºC]
v	Specific volume	[m^3/kg]
η	Plant net efficiency	[%]

[1] If no other units are mentioned in the text, the following units are used.

1 Introduction

The climate goal of limiting warming to 2 °C is becoming more difficult and more costly with each year goes by (International Energy Agency, 2012). Intensify policies that support environmental protection in a global context, particularly in terms of reducing greenhouse-gas emissions are currently of importance. Securing future energy supplies and mitigating their environmental impact are crucial issues because of their direct contribution to climate change.

Representing 41 % of the carbon emissions in 2010, the power sector is the largest contributor in terms of CO_2 emissions (International Energy Agency, 2012). Measures that raise the cost of fossil fuels such as establishing CO_2 price, leads to an increase of the value of energy efficiency in power generation. Currently there are many inefficient power plants in operation around the world that contribute to higher emissions. There are also policies to reduce pollution from power plants in operation, which can have the secondary effect of closing these inefficient plants.

Nowadays, the combined cycle gas turbine (CCGT) represents a high percentage of the total electric power generation, among the plants that produce electricity from fossil fuels. Compared to thermoelectric plants, they offer a higher efficiency and acceptable CO_2 emissions.

The global CO_2 emissions due to fossil-fuel combustion reached 31.2 gigatonnes in 2011, number which corresponds to the highest value in years (International Energy Agency, 2012). The CO_2 concentration has increased over last years, and this tendency of growing need to be mitigated. This is the reason why the interest in using low-carbon and high-energy-efficiency technologies are in the spotlight.

The suggestion of a new technology that is well suited for CO_2 capture becomes interesting if the objective is to put the energy production in a more sustainable path. In this sense, this technology represents an advantage over the extended CCGTs. The recent proposal consists in an air breathing semi-closed recuperated cycle (SCRC) which, although it has been proposed since the 1980s, has not yet been practically developed.

1.1 Formulation of the problem and objectives

In an electrical market in which CCGTs are widely extended and where the interest of low CO_2 emissions is growing, a technology that permits the CO_2 capture has a crucial importance in the future. The SCRC technology can cover these environmental interests while offering a high

efficiency, being a competitive alternative to CCGTs. The possible advantages of the SCRC over CCGTs results are an interesting topic for investigation.

The primary objective of this thesis is to compare the extended CCGT technology with the innovative SCRC by using the simulation tool EBSILON®Professional. The other goals of the work are listed below:

- A literature study of CCGTs, pressurized HRSGs and SCRCs.
- Design, simulate, and validate the two cycles proposed.
- Develop a sensitivity analysis of the SCRC.
- Compare and evaluate the results obtained in the simulations and the sensitivity analysis.
- Propose future work and the challenges with the SCRC technology.

1.2 Risk assessment

Any risk assessment for the work regarding this thesis has been required due to the fact that during the writing there have not been performed any laboratory work or excursions.

1.3 Contribution work

The main contributions of this thesis are listed below:

- Modeling and simulation with EBSILON®Professional of a CCGT and a SCRC.
- Give illustrative but not exact values of a SCRC cycle.
- Analysis of the influence of different variables of the SCRC such as changes in turbomachinery's efficiency.
- Analysis of the results and list of the advantages and inconveniences that SCRC technology might provide.

1.4 Limitations

The results of this study are limited to electricity generation in onshore cases. The assumptions and hypothesis made and the simulation software have influenced the results obtained, and some of them might be reviewed.

1.5 Structure of the report

The report is structured in four different parts.

1. Theoretical part. In this part, the CCGT and SCRC technologies, and a proposal of a pressurized HRSG are described. It also includes a first comparison of such cycles, as well as the modelling of the proposed thermodynamic cycles.
2. Simulation and results. In this part the results obtained in the simulations of the cycles modelled are presented, analyzed and compared.
3. Sensitivity analysis of the semi-closed recuperated cycle.
4. Conclusion. The last part of the report includes the challenges, potential and future work for the SCRC technology.

2 The combined cycle gas turbine

2.1 What is a combined cycle gas turbine

A combined gas turbine and steam cycle (CCGT) is the union of two thermal power cycles. Nowadays, the combination used for commercial power generation is a gas-topping cycle with a steam-bottoming cycle which operates at lower temperature level than the gas cycle (Kehlhofer et al., 2009). The Brayton cycle corresponds to a gas turbine, whereas the cycle corresponding to a conventional steam turbine is the Rankine cycle. Both technologies are connected by a heat recovery steam generator (HRSG).

Currently, a combined cycle gas turbine is capable of achieving a net power efficiency close to 60 % (Bolland, 2009).

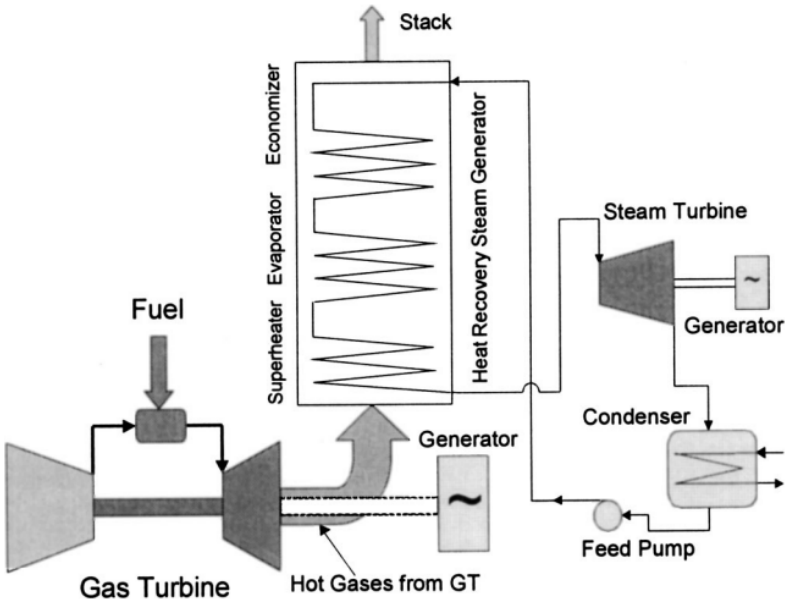

Figure 2.1 Common combined cycle gas turbine plant (Zwebek and Pilidis, 2003)

Figure 2.1 shows the simplest combined cycle configuration. As it can be appreciated, atmospheric air is taken by the gas turbine (GT). The air is compressed in a compressor, and afterwards it is mixed with the fuel in the combustor chamber. The exhaust gases are expanded in a turbine, which is connected to a generator and electricity is produced.

The HRSG uses the heat from the high temperature of the flue gas in order to raise steam. The steam raised supplies a steam turbine with the aim of generating additional electric power. After the turbine there is a condenser and a feed pump which impulses the water to the HRSG again.

The most common tendency is to couple the gas turbine and the steam turbine to a common shaft, so that jointly drive the same generator.

2.2 Main components

2.2.1 Gas turbine

A simple gas turbine (GT) is comprised of three sections: a compressor, a combustor and a turbine. The typical net efficiency for large GT used in power plants is in the range 35-40 % (Bolland, 2009).

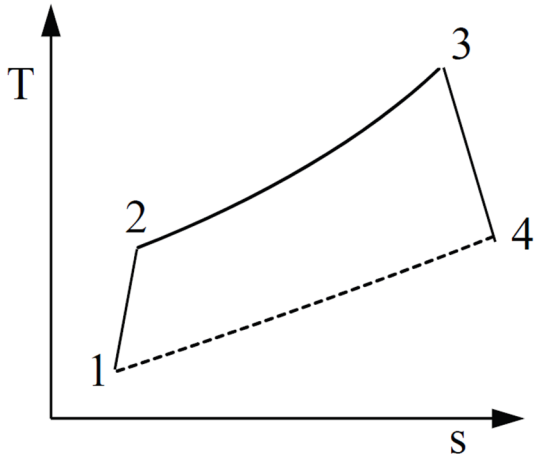

Figure 2.2 Temperature – entropy diagram of a gas turbine. Processes: 1→2 compression (power required); 2→3 combustion; 3→4 expansion (power generation). The turbine typically generates twice the power consumed by the compressor (Bolland, 2009).

A GT operates on the principle of the open Brayton cycle (Figure 2.2). First the air is compressed to a pressure of 14 to 30 bar, depending upon the gas turbine used (Kehlhofer et al., 2009). The compressed air burns the fuel in the combustor chamber, producing a hot gas with a temperature normally higher than 1000 ºC (Kehlhofer et al., 2009). Finally, the hot gas is expanded in the turbine, which drives the compressor and the generator. The hot gas leaves the turbine at slightly above atmospheric pressure, and with a temperature in the range 450-650 ºC (Bolland, 2009).

It is worthwhile to comment the operation of the turbine. First, the pressure energy contained in the hot gas is converted to kinetic energy thanks to the stator. Then the kinetic energy is converted to power due to the rotation of the shaft. This conversion takes place in the rotor, which is connected to the generator (Bolland, 2009).

Turbine inlet temperature

This temperature depends upon the type of GT used, and it is preferably as high as possible in order to obtain high cycle efficiency and specific power[2]. This temperature is limited by the materials and the cooling system of the GT. With the aim to limit the turbine inlet temperature (TIT), the combustion takes place with an excess air ratio between 2.5-3.0 (Bolland, 2009).

Fuels for gas turbines

Natural gas (NG) is the most common fuel used in gas turbines. Around 80 % of installed gas turbine capacity use NG, while approximately 18 % are operated on light oil and distillates, and 2 % use residual oil (Bolland, 2009).

The lower heating value (LHV) is an important property of the fuel. This number corresponds to the magnitude of the enthalpy of combustion obtained when all the water formed by combustion is vapor (Moran and Shapiro, 2006). This value defines the mass flow of the fuel which has to be supplied to the GT. Thus, the GT efficiency is influenced by the LHV.

From a technical point of view, gaseous hydrocarbon fuels are more beneficial than liquid fuels with respect to plant performance, pollution emission levels and plant availability. There are fuel specifications for GT in order to prevent high temperature corrosion, fuel system problems and ash deposition (Bolland, 2009).

In that respect, NG with little sulphur content and no fuel-bound nitrogen is the best option. CCGT are also able to burn liquid fuels with the aim of producing when NG is not available or to better negotiate the NG price.

2.2.2 Heat recovery steam generator

As its name suggests, the aim of the HRSG is to produce steam while the flue gas temperature is reduced. The temperature and pressure of the steam produced in a combined cycle with NG as fuel vary respectively in the range 450-460 ºC and 30-170 bar (Bolland, 2009).

There are many alternative configurations of an HRSG. Normally the configuration of the steam cycle depends on design criteria such as cost, type of application, performance or efficiency. In large combined cycle plants (400-500 MW), the cycle is usually designed with a triple-pressure reheat steam, which permits to use lower temperatures of the flue gas. This reduce the flue gas temperature to around 80 ºC (Bolland, 2009) and the efficiency of the combined cycle.

[2] The relation between the gas turbine net power output and the air flow rate is known as specific power.

Simple-pressure HRSG description

The simplest configuration is explained here. It consists in a simple-pressure HRSG. In this case the HRSG has three different heat exchange sections which transfer the heat from the hot exhaust gas to the water/steam cycle.

Firstly, the subcooled water is pre-heated in an economizer to near its saturated estate. The water is not at saturated conditions in order to avoid evaporation in the economizer at off-design conditions. Obviously, this saturation temperature depends on the pressure of the water flowing though the exchanger. Afterwards, the water is lead to a boiler/evaporator. Here the water is evaporated at constant temperature and pressure. At the end, the steam from the evaporator is heated up in a superheater, and its enthalpy is increased.

There are two main reasons for superheating the steam before entering into the steam turbine. Firstly, to accomplish the limit of moisture content at the steam turbine exit and reduce the risk of erosion. Secondly, because the presence of liquid in the turbine could reduce the power output by slowing down the blades (Kehlhofer et al., 2009). Moreover, superheating is interesting for increasing the TIT, which depends strongly on the enthalpy at high pressures. An increase in the TIT contributes to an increase of the steam turbine power output.

TQ diagram

The profiles for the heat transfer process between the water/steam and the flue gas are usually illustrated in a TQ-diagram. The three different zones of a single-pressure HRSG commented above are indicated in Figure 2.3.

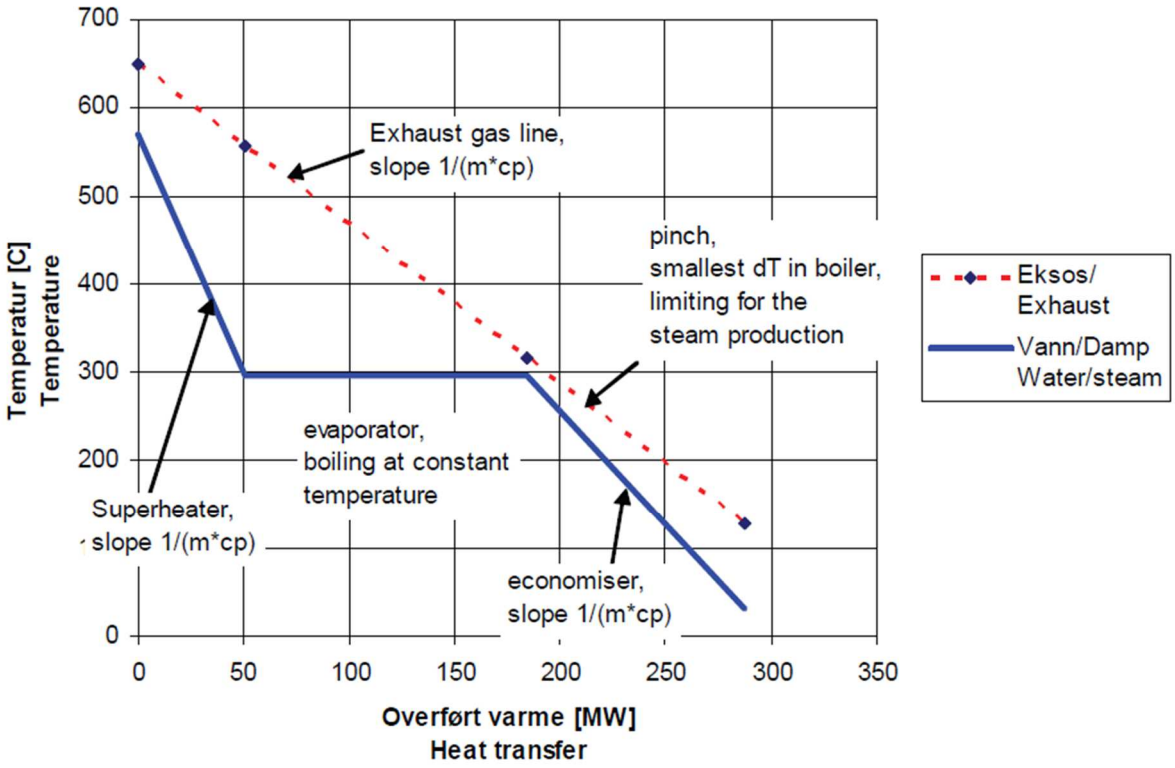

Figure 2.3 TQ diagram for a single-pressure HRSG (Bolland, 2009)

A relevant parameter is the so-called pinch point. It is defined as the minimum temperature difference between the exhaust gas and the water within a given pressure. It is important the location of the pinch point because it limits how much steam can be produced. It depends on the flue gas inlet temperature into the HRSG and the pressure of the water/steam.

Much of the heat transfer area is situated near the pinch point. The pinch point is inversely over-proportional to the heat transfer area. This means that with lower pinch points, the area is higher but the exhaust heat is used better and more steam is generated. For high-efficiency plants, pinch points are often in the range 8-12 K (Bolland, 2009).

Pressure drop

The pressure drop in the HRSG is compensated by an increase of the pressure at the gas turbine outlet. Therefore, the gas turbine produces less work. This means that the power generation in the gas turbine is very sensitive to a change in the pressure drop of the HRSG.

2.2.3 Steam turbine

The steam produced in the HRSG is expanded in a steam turbine (ST) to around 40 mbar (Bolland, 2009). In the turbine, some of the energy of the steam is converted to power. The work carried out by the ST depends on the enthalpy difference between the inlet and outlet of the turbine.

Lower exit pressures are preferred due to the increase of the ST power output. Nevertheless, this pressure is limited by the type of cooling system used in the CCGT. On the other hand, the steam temperature before entering into the ST is in the range 450-570 ºC. The largest temperature value is limited by the material of the ST.

As combined-cycle plants habitually generate steam at more than one pressure level, the ST has multiple inlets depending upon the number of pressure levels. For instance, in the case of an HRSG with three-pressure levels and reheat, the ST will have three inlets, two outlets and one crossover.

The type of steam turbine used depends on the usage of the generated steam. Much more interesting for this thesis, the condensing steam turbines are used for power generation.

Moisture content

The percent moisture can be defined as the ratio of the mass of liquid to the total mass of the steam, and it represents the quality of the steam (Moran and Shapiro, 2006). A common practice is to maintain at least 87 % quality at the turbine exit (Bolland, 2009). This permits to avoid erosion in the turbine blades. If the steam passing through the turbine has a moisture content too high, the liquid droplets can erode the turbine blades, with the consequently decrease in the turbine efficiency and an increase of the need for maintenance.

Reheat

After the expansion of the steam in the high-pressure ST, it is normally reheated in the HRSG before further expansion. This practice permits advantageous operating pressures in the boiler and condenser, and yet offset the problem of low quality of the steam at ST exit.

2.2.4 Cooling system

The cooling system of a CCGT has the function of condensing the steam by heat transferring from the steam to the cooling fluid. There are three fundamentally cooling configurations:

- Evaporative cooling with wet or hybrid cooling tower
- Once-through water cooling using river water or sea water
- Direct air cooling in an air cooled condenser

Habitually, the type of cooling system used in a CCGT depends on the available supply of cooling water because the once-through water-cooled condenser is often the most economic cooling technology. In this case, after the water has served as a heat sink, it is returned to the water source (river, sea, or cooling pond) from which was taken. The maximum increase of the cooling water temperature that flows through a condenser is normally in the range 10-15 K (Bolland, 2009).

2.2.5 Feedwater tank and deaerator

The condensed water is pumped to a higher pressure until the feedwater tank. Here the condensed water is mixed with makeup-water in order to cover the leakages through the steam cycle. Normally the mixed water is heated up in the HRSG, and afterwards it enters into the deaerator.

The deaeration is the removal of non-condensable gases such as CO_2 and O_2 from the water or steam. Its function is very important because these components can cause corrosion of the devices and piping. It utilizes two different principles: the first one is the fact that the solubility of a gas in a solution decreases when the temperature increases; the second one is the Henry's Law, which affirm that the gas solubility in a solution decreases when the gas partial pressure above the solution decreases (Bolland, 2009).

2.3 Emissions

By producing in a CCGT using NG as fuel, carbon dioxide (CO_2) and nitrogen oxides (NO_x) are the mainly emissions which can negatively affect the environment (see Table 2.1). Concentration levels of these substances in the exhaust gas depend on the fuel composition. Sulfur dioxide (SO_2) emissions usually are negligible because of the general low content of sulfur in the NG. The high excess air ratios typical of GTs enables practically a complete combustion, which leads to a very low level of unburned constituents such as carbon monoxide (CO) or unburned hydrocarbons (UHC) (Lieuwen and Yang, 2013).

Table 2.1 Typical emissions of a CCGT without CO_2 capture (Rao, 2012)

SO_2 emissions (g/MWh)	negligible
NO_x emissions (g/MWh)	84.8
Particulate matter emissions (g/MWh)	negligible
CO_2 emissions (kg/MWh)	372.0

Regarding heat emissions, thermal energy is rejected to the environment through stacks, condensers, and off-gases. Noise emissions are not considered as a problem from a technical standpoint, because of the currently available acoustic insulation technology (Bolland, 2009).

3 The pressurized heat recovery steam generator

After a long literature study regarding pressurized heat recovery steam generators, it was found that a patent related to this topic developed by Natural Resources Canada (NRCan) was filed in 2008 (Clements, 2009). In this patent a direct pressurized combustion process for Steam Assisted Gravity Drainage (SAGD) proposals is described.

The technology developed consists in a direct pressurized combustion process. In this process, the combustion takes place with nearly pure oxygen as oxidizer (oxy-fuel combustion) and at high pressures in the range of 100 bar or higher (Canada's Oil Sands Innovation Alliance, 2015). The stream generated is composed basically of CO_2 and steam due to the combustion characteristics and the recycled flue gases (Cairns, 2013).

After the combustion process, the products of the combustion are lead to a direct contact steam generator (DCSG). In this device, steam is produced by directly contacting water with the hot and pressurized gas, causing the evaporation of this water. Hence, the need to use boiler tubes as in common steam generators is avoided.

After this, the SAGD would take place. The SAGD practice consists in pumping this flue gas obtained underground in order to aid in bitumen extraction (Clements, 2009). This part would not be explained because such information is beyond the scope of this project.

It is worthwhile to mention that the combustion could take place with air, but this practice has the disadvantage that the steam produced has lower quality due to the fact that the flue gas contents nitrogen, which leads to a decrease of the heat available for evaporation of water (Cairns, 2013).

As the pressures in such technology are considerably high, it was necessary to prove whether direct steam generation was possible in a pressurized environment. And NRCan was the company who brought this project. Early, pilots were developed to the member companies of Canada's Oil Sands Innovation Alliance (COSIA), which is working in the testing of DCSG technology with actual SAGD-produced water (Canada's Oil Sands Innovation Alliance, 2015).

It can be concluded that the DCSG is an alternative to the existing heat recovery steam generators. Researchers are currently testing the high pressures in this new technology. For instance, CanmetENERGY is developing the steam generation technology known as the High Pressure Oxy-fired direct contact steam generator (HiPrOx/DCSG) (Cairns, 2013).

4 The air breathing semi-closed recuperated cycle

4.1 Overview of the semi-closed combined cycles

The supercharging concept it is not a novelty idea. This practice permits to operate at elevated compressor inlet pressure with the advantage of a higher power density. It is widespread applied in Diesel and Otto motors. However, supercharging is currently not used for thermal power generating cycles despite the important role that played the closed cycles in this field.

The supercharged cycles' history started in 1939 with the commercialization of the closed cycle gas turbines, which had the capability to use dirty fuels due to the fact that the heat is transferred via heat exchanger to the cycle fluid (Wettstein, 2013). This machinery still has a potential for technologies such as solar or nuclear, in which temperature limitation of the heat exchanger does not matter. For other applications where overcoming this temperature was necessary, the idea of the semi-closed cycles with internal combustion appeared around the 1940s (Wettstein, 2013). The concept semi-closed refers to the fact that most of the flue gas is recirculated, whereas the excess gas is removed.

These cycles use a fluid circulation in a closed loop, and therefore supercharging is possible. An internal combustion fed with injected oxidizer and fuel generates their heat input.

In the 1980s, limiting CO_2 emissions came into the focus (Wettstein, 2013). This is the reason why using a semi-closed cycle with internal and near stoichiometric combustion (so-called oxyfuel cycles) became interesting. Such cycles permit to process the remaining CO_2, or the carbon capture and storage (CCS). Even though the production of technically pure oxygen is expensive, the oxyfuel cycles are only economic when burning a fuel with high carbon content.

The use of ambient air as oxidizer in the semi-closed cycle with internal combustion was also an attractive idea at that time. Working with air allows a high power density and a power control by changing the pressure instead of the temperature.

More recently, the absorption of CO_2 from the exhaust gas of existing CCGTs was developed. As in an open cycle gas turbines the concentration of CO_2 in the exhaust gas is low, a recirculation of cooled exhaust gas into the compressor (EGR) has been suggested (Bolland and Sæther, 1992). At a given flame temperature, this practice reduces NO_x formation rate in the combustor.

Finally, the air breathing supercharged semi-closed cycle were firstly developed by a group of engineers from the University of Florida. Since the late 1990s, they have been working on two

variations of an air breathing supercharged semi-closed cycle. The basic cycle is called HPRTE (high pressure regenerative turbine engine), and the other, which incorporates a refrigeration loop, is named PoWER (power, water extraction and refrigeration) (Wettstein, 2013).

The idea used in this current thesis about an air breathing semi-closed recuperated cycle (SCRC) for electric power generation is subject to the one suggested by H.U. Frutschi (2005). Later on, different cycle options of the SCRC allowing CO_2 absorption were patented (Wettstein et al., 2010).

Last years, descriptions of the SCRC and its additional opportunities have been published in different papers (Enge et al., 2006, Wettstein, 2013, Wettstein, 2014b). The application of such cycle for naval propulsion also has been recently explored (Wettstein, 2014a).

4.2 What is an air breathing semi-closed recuperated cycle

Frutschi's basic idea (2005) of an air breathing semi-closed recuperated cycle (SCRC) is illustrated in Figure 4.1. A detailed description of the cycle is presented in Chapter 6.

The charger group ATL2 sucks up atmospheric air into the closed loop and also expands the excess of the flue gas to ambient pressure. The main group ATL1 operates at a high pressure level and drives the main generator, producing power. A large part of the main turbine exhaust gas is constantly recirculated. Thus, a low oxygen and high-CO_2 concentration in the stack is reached. This is lately useful for driving a CO_2 absorption (Wettstein, 2013).

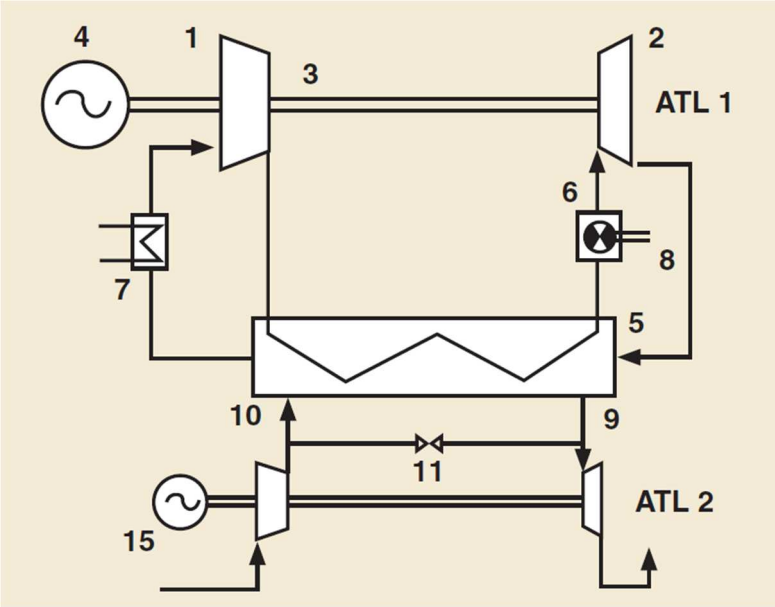

Figure 4.1 Basic SCRC scheme of the Frutschi patent. Key features: (1) compressor; (2) turbine; (3) drive shaft; (4) main generator; (5) recuperator; (6) combustor; (7) after-cooler; (11) bypass valve

The pressure vessel

Recently, the pressurized part of the SCRC arrangement in a common pressure vessel has been proposed (Wettstein, 2013). Regarding the main generator, it can be arranged in the vessel as seen in Figure 4.2, or a shaft sealing can be used and arrange the generator outside the vessel.

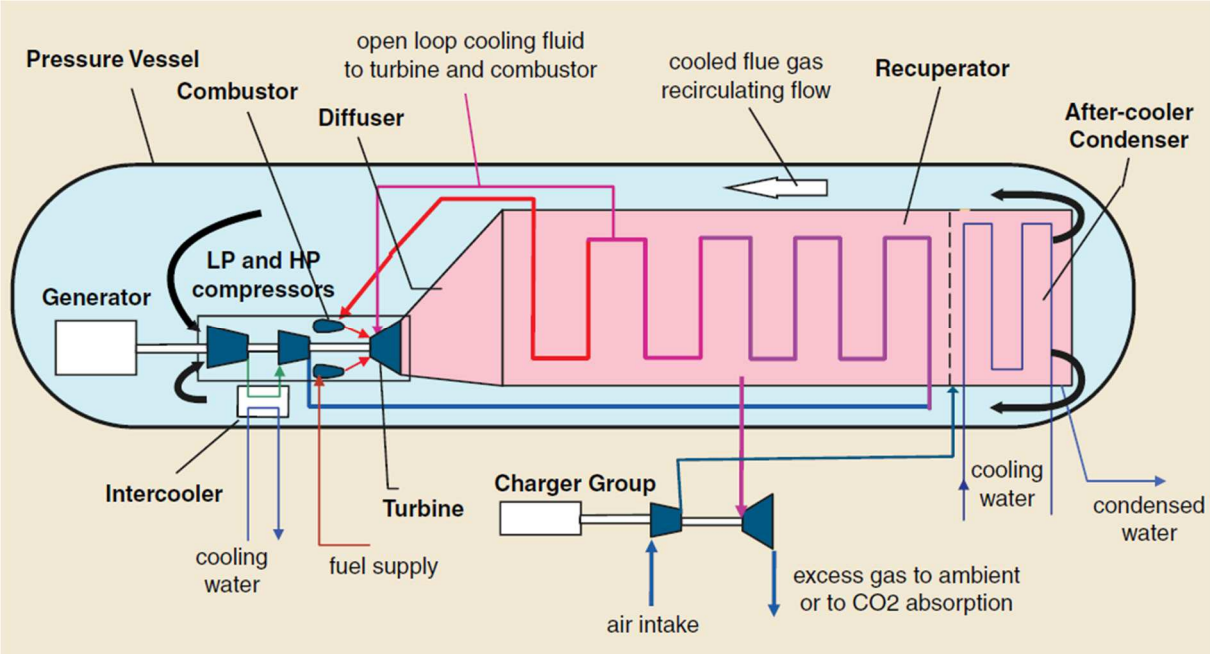

Figure 4.2 SCRC arrangement in a common pressure vessel (Wettstein, 2013)

This suggestion is useful in order to attenuate the high pressure of the casings. As the vessel operates at the pressure at the charger compressor outlet, which can take values around 4-6 bar, it sees internally only the low temperature of the after-cooler discharge. Strictly speaking, the vessel is exposed to nearly ambient temperature internally and externally, and therefore the need for a heat resistant design or insulation is avoided. The use of a vessel also simplify the design of the recuperator, which has only to be designed taking into account its own pressure drop.

4.3 Main components

First of all, it is worthwhile to mention that the characteristics of this flue gas circulating through the devices has to be taken into account when designing the machinery and pipes.

The SCRC is composed by two different parts which are connected by the recuperator.

The so-called charger group arranges a charger compressor and a discharge turbine connected to a generator, which permits to produce electric power. As these machines work at low pressures, current turbomachinery can be used in this part.

The second part is the pressurized group, which includes an after-cooler, a compressor, a combustion chamber and a turbine. The turbomachinery operates at considerably high pressures and with lower pressure ratios compared to GTs. Hence, turbochargers or micro-turbines can be useful (Frutschi, 2005), but they have to be designed to support thermal and pressure stresses. Regarding the after-cooler, it also has to be designed to support high pressures. Finally, it is worthwhile to comment the combustor design. It must operate with an oxidizer inlet temperature in the range 850-900 ºC. This is the reason why one of the best options is to use the second combustor in sequential combustion gas turbines (Wettstein, 2013). These combustors can operate at an even higher oxidizer temperature level and with low oxygen content (Guethe et al., 2011).

The element that connect both loops is called recuperator. It is defined as a type of heat exchanger in which a liquid or gas is separated from another gas or liquid by a wall. In this case the heat is exchanged between two gases. The energy from the hot gas is conducted by this wall to the cold gas (Moran and Shapiro, 2006). These recuperators can take different forms such as the ones shown in Figure 4.3. There is an open issue regarding the recuperator design, because it has to support high pressures and temperatures. Therefore this device has to be designed with resistant materials.

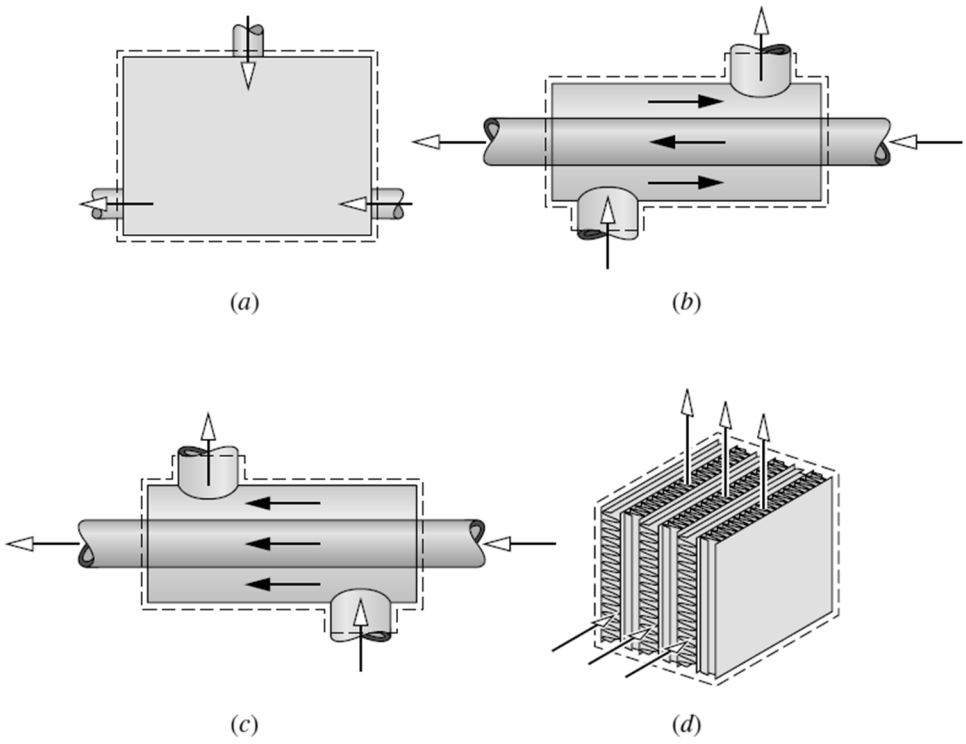

Figure 4.3 Common heat exchanger forms. (*a*) Direct contact; (*b*) tube-within-a-tube counterflow; (*c*) tube-within-a-tube parallel flow; (*d*) cross-flow (Moran and Shapiro, 2006)

4.4 Fuels and emissions

As it occurs in CCGTs, any gaseous or liquid hydrocarbon can be used in this technology (Enge et al., 2006). A study using a liquid as fuel was carried out by Wettstein (2014a).

The emissions will depend on the fuel used. But using natural gas might be one of the best possibilities, at least for onshore electricity production. Due to the near stoichiometric combustion that takes place in the combustor, a small content of O_2 in the flue gas is detected, while the CO_2 concentration is substantially high. The recirculation of the flue gas in the main loop leads to a high content of N_2. A typical composition of the exhaust gas is presented in Table 4.1.

Table 4.1 Typical SCRC's exhaust gas composition (Wettstein, 2013)

Ar mass fraction (%)	1.32
N_2 mass fraction (%)	77.29
O_2 mass fraction (%)	1.56
CO_2 mass fraction (%)	15.17
H_2O mass fraction (%)	4.67

These are therefore the main emissions of the SCRC when burning natural gas. In the table presented above NO_x, particulate matters and unburned hydrocarbons were not considered. The concentration of UHCs might be higher compared to CCGTs because of the low air excess at which the combustion takes place. The high content of N_2 in the burnt gas might produce more NO_x than in a CCGT plant. Although these components in the discharged gas are probably more concentrated than in a CCGT, the low amount of fluid discharged leads probably to low emissions per kW generated.

Regarding the CO_2 content in the excess gas, carbon capture and storage (CCS) finalities, such as CO_2 absorption (Wettstein, 2013) are options that lead this technology to almost zero-CO_2 emissions.

And finally, noise and heat emissions are also presents in this cycle. The first one is easy to solve by using current acoustic insulation technology.

5 Main differences between a common CCGT plant and the proposed SCRC plant

In order to understand both technologies, besides from understanding how they operate, it is important to know the main differences between them.

One of the most important difference is the type of thermodynamic cycle that takes each technology. A CCGT is composed of two different thermodynamic cycles: the Brayton cycle (GT), which in this case operates as an open cycle, and the Rankine closed cycle, which corresponds to the steam turbine. The open cycle renews the working fluid every cycle, whereas the closed cycle reuses the fluid continuously.

Contrarily, the SCRC consists of one thermodynamic cycle: it is called a semi-closed cycle. Such cycle recirculates nearly the 70% of the working fluid (Wettstein, 2013). The excess of gas is discharged out of the closed loop and fresh air is mixed with the recirculated flow mentioned above. One consequence of this recirculation is that the inlet air flow rate needed in this cycle is approximately 2.5 times lower than in a common CCGT (Wettstein, 2013, Wettstein, 2014b). Thus, the SCRC has a high specific power related to the inlet air rate.

Furthermore, it is easy to realise that each technology uses different machinery.

Firstly, if the main group of a CCGT plant is compared with the supercharged part of a SCRC plant, there are several differences that have to be considered.

The gas turbine used in a CCGT plant encompasses a chamber combustor, a compressor and a turbine that drives the generator through the shaft. After the turbine, there is the HRSG used for steam generation. All these machines work at low pressure. The main group of the semi-closed cycle includes the compressor, the recuperator, the combustor, the turbine, the drain, and the after-cooler. As all of this machinery work at high pressure, the characteristics of these components cannot be the same as the ones used in common CCGT.

On the one hand, this supercharged part uses turbocharger or micro-turbine components instead of the conventional turbines and compressors. There are two main reasons for using such turbomachinery: the high pressure of these components, and the low pressure ratio.

Concerning the recuperator of a SCRC, its function is to heat up the fluid work before entering in the combustor. Producing steam is the function of the HRSG. It is worthwhile to comment that in the recuperator the pressures and temperatures are notably higher than in an HRSG.

The CCGT plant's condenser works at low pressure, and it condenses all the working fluid, which in this case is water. In contrast, the SCRC's after-cooler operates at high pressure, and the fluid that is cooled down is a mixture of water, exhaust gas and air. Only the water from the mixture is condensed and, afterwards, it is drained.

In these two last cases, the heat exchangers and the after-cooler need to be recovered by heat-resistant materials, which have the aim of supporting the high pressures and temperatures.

It is also significant the sizes of the recuperator and the after-cooler. As a result of the high pressure in these devices, the heat transfer coefficients are increased. Consequently, less area is needed to transmit the same amount of heat (Wettstein, 2013). The work of Enge et al. (2006) reveals that the recuperator and after-cooler sizes are approximately 2.5 times smaller than the HRSG and the condenser sizes of a CCGT plant.

Another machinery dissimilarity between both technologies resides in the combustor. The SCRC's combustor operates at high inlet temperature (Wettstein, 2013). It is the reason why the fuel is preheated using a fuel gas compressor, and the reason for using the second combustor in sequential-combustion GT (Wettstein, 2013). Furthermore, the SCRC's combustion is near stoichiometric conditions, and the CO_2 concentration of the exhaust gases is higher than in a conventional CCGT plant, which works with excess of air.

Finally, if the bottoming steam cycle from a CCGT plant is compared with the charger group of a SCRC, there are also some dissimilarities that have to be considered. The most important difference is that in the semi-closed cycle, instead of the steam turbine and the conventional condenser that constitute the CCGT bottoming cycle, there are a charger compressor and a discharge turbine. The charger compressor can be the same as the one used in a common CCGT, because of the similar inlet pressure (Wettstein, 2013). The discharge turbine could be the same as the one used in a CCGT plant, but taking into consideration that the compression ratio is lower and the gas flow that flows through the turbine has a higher content CO_2.

Table 5.1 sums up the main dissimilarities commented above as well as others, and it gives representative data for each plant.

Three different sources (Bolland, 2009, Kehlhofer et al., 2009, Wettstein, 2013) have been used in order to obtain the CCGT-quantitative values. SCRC-quantitative numbers are built on the study done by Wettstein (2013). The order of magnitude of these values are the same as the data obtained in other similar studies such as Enge (2006) and Wettstein (2014b).

Table 5.1. Main differences between a common CCGT and the proposed SCRC

	CCGT	**SCRC**
Number of thermodynamic cycles	2	1
Steam cycle	Yes	No
Sort of thermodynamic cycle	Brayton open cycle Rankine closed cycle	Semi-closed cycle
Net thermal efficiency[3]	**60.0 %** (at full plant output)	**54.5 %** (with bottoming cycle to 62 %)
Specific power related to the inlet air rate (kJ/kg)[4]	**700**	**1450**
Turbomachinery volume reduction factor[5]	**1**	**2-3**
Recirculation factor (%)	0.0	70.6
Main compressor flow	Fresh air	Fresh air + exhaust gases
Main compressor inlet pressure (bar)	1	6
Main compressor pressure ratio	**19-35**	**8-12**
HRSG/recuperator function	Steam production	Heating up the fluid work before entering in the combustor
HRSG/recuperator hot end temperature difference (K)	20-40	8
Heat exchange requirement in HRSG/recuperator related to the power output (%)[6]	100	131
Fuel compressor	Normally not necessary for natural gas fuel	Needed for high load, but not at part load below 50% power
Fuel preheat temperature (ºC)	-	250
Oxygen excess factor in combustor	**2.2-3.0**	**1.1**
Combustor pressure (bar)	19-35	54
Exergy loss in combustion (%)	25	22
Ar molar fraction in exhaust gas (%)	0.90	0.96
N_2 molar fraction in exhaust gas (%)	74.94	80.09
O_2 molar fraction in exhaust gas (%)	12.91	1.42
H_2O molar fraction in exhaust gas (%)	7.40	7.53

[3] The net thermal efficiency η is given by $\eta = W_{net,plant}/(\dot{m}_{fuel} \cdot LHV)$ where $W_{net,plant}$ is the net power developed by the plant, $\dot{m}_{fuel}$ represents the fuel consumption, and LHV is the lower heating value of the fuel.

[4] The specific power related to the inlet air rate is given by the relation $W_{net,plant}/\dot{m}_{air}$ where $W_{net,plant}$ is the net power developed by the plant and $\dot{m}_{air}$ represents the inlet air rate.

[5] ENGE, Y. O., WIRSUM, M. & WETTSTEIN, H. E. 2006. The Potential of Recuperated Semiclosed CO_2 Cycles. *ASME Turbo Expo 2006: Power for Land, Sea, and Air*. Barcelona, Spain: American Society of Mechanical Engineers.

[6] The heat exchange requirement in HRSG/recuperator related to the power output is given by $Q_i/W_{net,plant}$ where Q_i is the heat power necessary in the HRSG/recuperator and $W_{net,plant}$ is the net power developed by the plant.

	CCGT	SCRC
Carbon dioxide molar fraction in exhaust gas (%)	**3.84**	**10.01**
Hot gas density at main turbine inlet (kg/m^3)	4.2	10.0
Main turbine exit temperature (ºC)	450-650	860
Main turbine exit pressure (bar)	1	54
Condenser/after-cooler pressure (bar)	0.04	54.00
Heat exchange requirement in condenser/after-cooler related to the power output (%) [7]	63	76
HRSG/discharge turbine outlet temperature (ºC)	**90**	**270**

[7] The heat exchange requirement in condenser/after-cooler related to the power output is given by $Q_i/W_{net,plant}$ where Q_i is the heat power exchanged in the condenser/after-cooler and $W_{net,plant}$ is the net power developed by the plant.

Considering the information above, it could be concluded that some of the advantages of the proposed semi-closed cycle are:

- The high specific power.
- The reduced size of the machinery.
- The characteristics of the exhaust gas discharged. The high CO_2-molar fraction in the exhaust gas and its high temperature permit to be better suited for the capture of CO_2.
- Less thermodynamic losses in combustion.
- High density at main turbine inlet.

Nevertheless, some disadvantages of the semi-closed cycle are listed below:

- The net-thermal efficiency approached is lower than the typical of a conventional combined cycle plant. This probably happens for three main reasons: the high heat exchange requirement relative to the power output (207 %) (Wettstein, 2013); the need of using additional machinery such as a fuel compressor; and the high temperature after the discharge turbine.

  However, it could be possible to improve the efficiency incorporating a bottoming cycle which utilizes the heat of the discharged gas.

- Another disadvantage is that the machinery of the pressurized group have to be recovered by resistant materials in order to support the high pressures and temperatures. This may increase the cost of these devices.

These advantages and disadvantages will be revised and amplified after the practical work.

6 Design and build process models

6.1 Description of the reference plant

The reference power plant is a typical dual-pressure combined cycle. As it can be appreciated in Figure 6.1, it consists of one large gas turbine from which the exhaust gas (2) is led to the heat recovery steam generator in order to produce steam. The distribution of economizers, evaporators and superheaters is made on the basis of literature references. This is, probably, not the most optimal distribution.

The steam is raised at two different pressures. The high-pressure (HP) steam (15) feeds the HP turbine. The expanded steam (16) is mixed with the low-pressure (LP) steam (10). The mixture (17) enters into the low-pressure turbine, where it is expanded. All this steam (4) goes through the condenser. The liquid water (5) is pumped at low pressure and it goes through the LP economizer.

At this point, the heated water (7) is separated into two different flows (8) and (11). The flow (8) is led to the low-pressure evaporator, and LP steam (9) is raised. Afterwards, it goes through the LP superheater, where it is heated up.

A second pump raises the pressure from (11). The pressurized water (12) is led to the HP-part of the HRSG, where HP steam is raised and heated up.

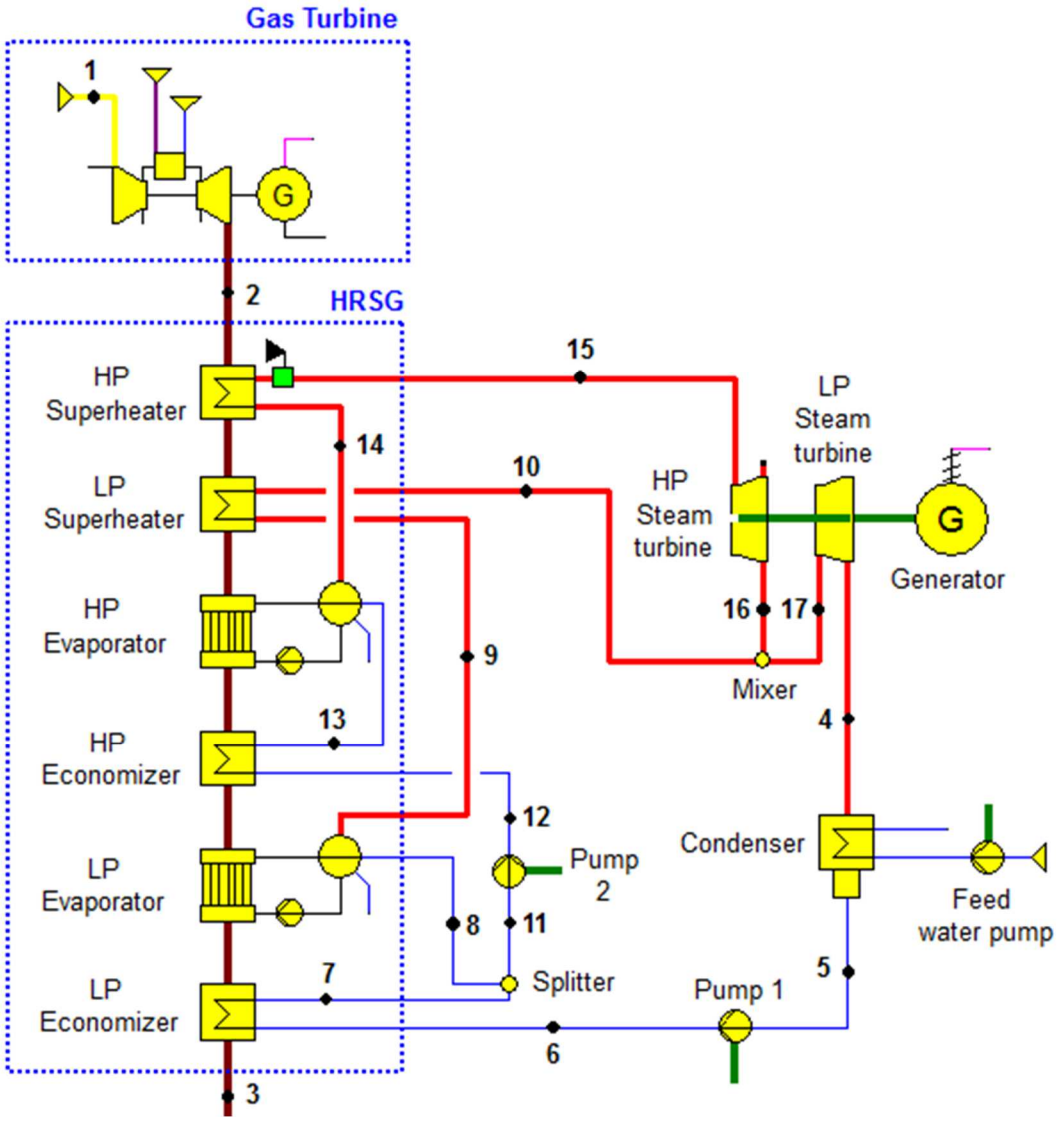

Figure 6.1 Scheme of the dual-pressure combined cycle gas turbine. Fluid type assigned to each pipeline: air=yellow, steam=red, liquid water=blue, gas=purple-red, flue gas=brown, electric line=pink, shaft=green.

6.2 Assumptions for the reference plant

The combined cycle gas turbine is designed for operating in onshore installations, and consequently with the requirements involved with it. In this case, a high efficiency and flexibility are the most important properties that the plant has to accomplish. Thus, the size of the turbomachinery, the investment cost and/or weight are not limited as in offshore applications.

For all these reasons, and on the basis of the literature sources, the AE94.3A is the model of gas turbine chosen for the simulation. This gas turbine is available in the VTU Library of the software used for simulating (EBSILON®Professional). The technical data for the gas turbine engine selected is summarized up in Table 6.1.

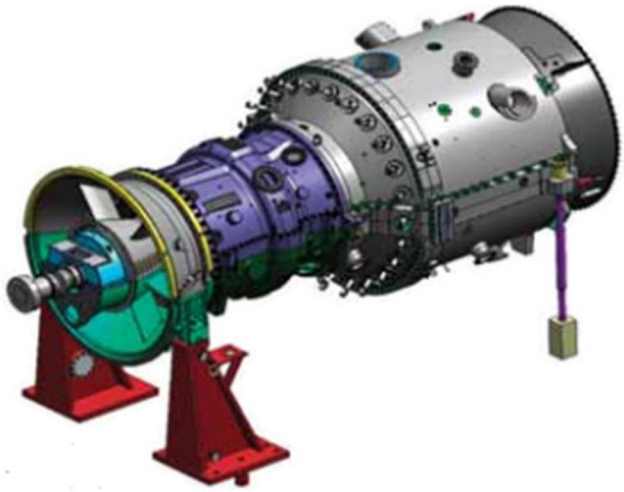

Figure 6.2 AE94-3A body (Ansaldo Energia)

Table 6.1 AE94-3A technical data (natural gas, ISO conditions, base load) (Ansaldo Energia)

Manufacturer	Ansaldo Energia
Gas turbine name	AE94.3A
Frequency (Hz)	50
Power output at generator terminals(MW)	294
Efficiency at generator terminals (%)	39.7
Heat rate (kJ/kWh)	9068
Exhaust gas mass flow (kg/s)	702
Exhaust gas temperature (ºC)	580.0
Cooling duty (MW)	0

The HRSG designed raises steam at two different pressures because of environmental reasons and efficiency. If a dual-pressure level is compared to an one-pressure level in an HRSG, the first one leads to a better exploitation of the heat of the exhaust gas, and the temperature of the gas when it is discharged into the atmosphere is around 70 ºC, instead of 100 ºC or more. A typical exhaust gas stack temperature in a high-efficiency plant is about 80-100 ºC (Bolland,

2009). Pressures chosen resemble the ones corresponding to San Severo combined cycle plant (Ansaldo Energia).

Another crucial assumption is the temperature before the HP steam turbine. It cannot be higher than 570 ºC due to material limitations. For this reason, this temperature is fixed at 560 ºC (Bolland, 2009).

The rest of values selected as inputs such as steam turbines efficiencies are based on theory about combined cycles (Kehlhofer et al., 2009, Bolland, 2009), and they are all indicated in Table 6.2.

Table 6.2 List of all the assumptions of the reference plant

Efficiency assumptions (all in %)	
HP steam turbine isentropic efficiency	88.0
LP steam turbine isentropic efficiency	88.0
Water pumps isentropic efficiency	80.0
Mechanical efficiency	99.6
Electrical efficiency	98.5
Temperature assumptions (all in ºC)	
Ambient temperature	15.0
Temperature at HP steam turbine inlet	560.0
External fuel delivery temperature	15.0
Cooling water temperature	15.0
Cooling water temperature after condenser	25.0
Limitation in exhaust gas temperature after HRSG	100.0
Pinch point temperature difference in evaporator	10.0
Pressure assumptions (all in bar)	
Ambient pressure	1.013
Exhaust gas pressure after GT	1.013
LP steam pressure	4.500
HP steam pressure	118.000
Steam pressure after LP turbine	0.040
External fuel delivery pressure	32.000
Cooling water pressure	2.000
Relative pressure drop assumptions	
Pressure drop in heat exchanger (flue gas path)	0.002
Pressure drop in heat exchanger (water/steam path)	0.050
Cooling water pressure drop in condenser	0.050
Pressure drop flue gas until atmosphere	0.045
Pressure drop at gas turbine intake	0.010
General cycle data assumptions	
Ambient air relative humidity (%)	60.0
LP superheater effectiveness (%)	80.0
Fuel LHV (kJ/kg)	50015

For the calculations, the model contemplates losses. Losses in the mixing point are unimportant due to the fact that the difference between mass flows mixed is high, ergo it is negligible. Heat losses are not included.

Argon (Ar), nitrogen (N_2), oxygen (O_2), steam (H_2O) and carbon dioxide (CO_2) are the gas-composition vectors considered for the calculations in the cycle. Regarding the fuel used in this model, pure methane (CH_4) is assumed and it is considered to be at external fuel delivery conditions (32 bar and 15 ºC). The air is at ISO conditions (see Table 6.3).

Table 6.3 ISO conditions

Sea level	
Temperature (ºC)	15.0
Pressure (bar)	1.013
Relative humidity (%)	60
Ar mass fraction (%)	1.28
N_2 mass fraction (%)	75.15
O_2 mass fraction (%)	22.90
H_2O mass fraction (%)	0.63
CO_2 mass fraction (%)	0.04

The table used for determining the water/steam properties is IAPWS-IF97. The formulation for the gas table considers real gas for N_2, O_2, Ar, CO, CO_2, SO_2, and FBDR formulation for the fuel gas. The air and exhaust gases are considered real gases.

6.3 Description of the semi-closed recuperated cycle

Two different variants of the semi-closed recuperated cycle have been considered: a first one with one intercooler in the main group (see Figure 6.3), and a second one with intercooling in the charger group and main group (see Figure 6.4). As both alternatives are very similar, the following detailed description corresponds to the variant with one intercooler.

The description of the cycle (Wettstein, 2013) follows in the sense of flow, starting at the compressor inlet.

Firstly, fresh atmospheric air (13) is compressed in the charger compressor. Then, this high pressure air flow (14) is mixed into the supercharged loop. The mixture (16) goes through the after-cooler, where it is cooled-down. Excess water from the mixture is condensed out.

After that, the high pressure cool fluid (1) is compressed in the main compressor. There is an inter-cooler between the LP and HP main compressors.

The flow (5) is heated up in the recuperator and afterwards it is mixed with the fuel in the combustor. The exhaust gases from the combustion (7) are mixed with a lower temperature gas (8) extracted from the high pressure path of the recuperator. This is done for supplying cooling systems of the combustor and the main turbine. The flow (9) is expanded in the main turbine, which drives the main compressor and the main generator.

The low pressure fluid from the main turbine (10) is led to the recuperator with the purpose of transferring heat to the high pressure fluid (5). Excess fluid (11) is discharged from the low pressure path of the recuperator into the discharge turbine, which drives the charger compressor and a second electric generator. Over there, the fluid is expanded and additional electric power is produced.

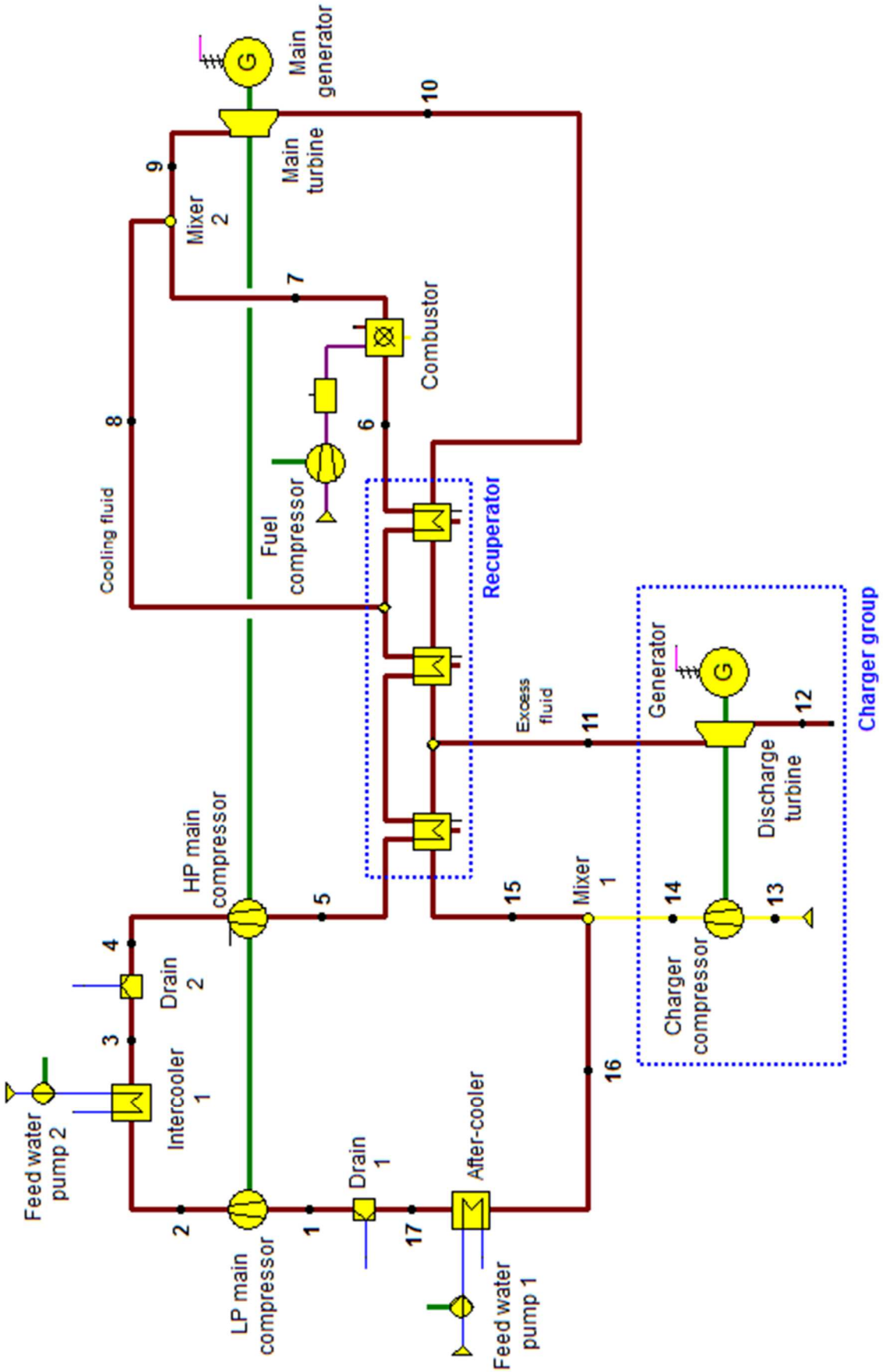

Figure 6.3 Scheme of the semi-closed recuperated cycle with one intercooler

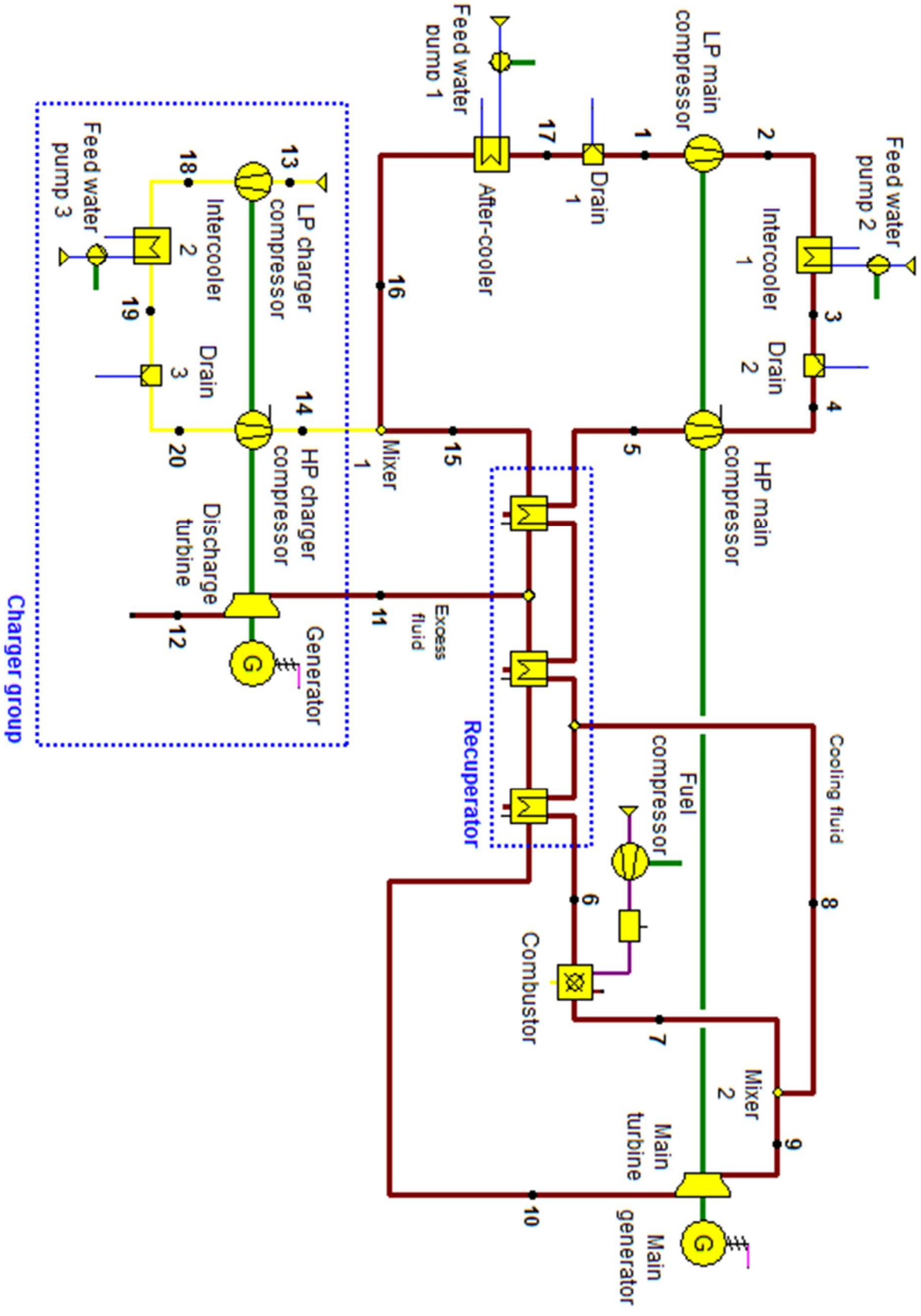

Figure 6.4 Scheme of the semi-closed recuperated cycle with two intercoolers. Compared to Figure 6.3, this option considers intercooling in the charger group.

6.4 Assumptions for the semi-closed recuperated cycle plant

The semi-closed recuperated cycle is designed for operating onshore. As it has been designed, the cooling fluid temperature is fixed at 550 ºC. This temperature depends strongly on the design of the recuperator, and consequently on the excess discharge fluid temperature. This is the reason why it will affect the subsequent sensitivity analysis done.

The design considers pressure losses in the different devices, additionally to mechanical friction losses in the turbomachinery, and generator losses. Inlet and outlet losses are considered extra with pressure drops. Pressure drops are considered as relative to the particular input pressure as percentages. The temperature drop by mixing fresh air into the semi-closed cycle is negligible because the differences between mass flows mixed are considerably big. Apart from this, losses in the cooling fluid mixing point are considered as part of the main turbine efficiency, which is considerably lower. The model does not incorporate heat losses.

Isentropic efficiencies are selected according to the current status of large commercial gas turbines, and taking in to account the ones assumed by Wettstein (2013, 2014b).

The turbine inlet temperature (TIT) is selected as 1600 ºC, as in the intercooled variant of Wettstein (2014b). The aim of this TIT value is to make easier the later validation of the results.

Due to the low content of oxygen in the gas circulating in the main loop, the oxygen excess in the combustor is considered 1.12. This lambda value corresponds to the safety margin for enough formation of oxide layers that protect the gas turbine environment (Wettstein, 2013).

Like in the reference case, Ar, N_2, O_2, H_2O and CO_2 are the gas-composition vectors considered for the calculations in the cycle. The air that entries into the cycle is at ISO conditions (see Table 6.3), and the fuel gas is pure methane (CH_4) at external delivery conditions (32 bar and 15 ºC).

The air and the flue gas are considered real gases for calculating their state values. Nevertheless, since real material values are not available for all real gases, FDBR gas table is used for the fuel. For water and steam lines, the table used is IAPWS-97.

When the net efficiency is calculated, auxiliary system power consumption (cooling water pumps) is not considered because it represents a small percentage of the thermodynamic power output (0.15 % for variant 1, and 0.22 % for variant 2).

All these assumptions affect the calculation of the net thermal efficiency (η), which has been defined as follows:

$$\eta\,(\%) = \frac{W_{net,plant}}{\dot{m}_{fuel} \cdot LHV} \cdot 100 \qquad \text{(Equation 6.1)}$$

where $W_{net,plant}$ is the net power developed by the plant in kW

$\dot{m}_{fuel}$ represents the fuel consumption in kg/s

LHV is the lower heating value of the fuel in kJ/kg

The fuel gas preheating temperature can be reached using heat extracted from the cycle. For this reason, extra heat injection is not considered in Equation 6.1. A calculation for corroborating this is done afterwards.

Table 6.4 contains the assumptions for this model. All these assumptions take into consideration the theory and literature about existing SCRC studies.

Table 6.4 List of the assumptions of the SCRC

Efficiency assumptions (all in %)	
Charger LP compressor isentropic efficiency	90.0
Charger HP compressor isentropic efficiency	90.0
Discharge turbine isentropic efficiency	90.0
Main LP compressor isentropic efficiency	91.0
Main HP compressor isentropic efficiency	91.0
Main turbine isentropic efficiency	86.0
Fuel gas compressor isentropic efficiency	83.0
Water pumps isentropic efficiency	80.0
Mechanical efficiency	99.6
Electrical efficiency	98.5
Combustion efficiency	99.0
Mass flow assumptions (all in kg/s)	
Air mass flow into charger compressor	266
Cooling water flow in intercooler	2500
Cooling water flow in after-cooler	2500
Temperature assumptions (all in ºC)	
Ambient temperature	15.0
Temperature at cooling fluid discharge from recuperator	550.0
Temperature downstream after-cooler	20.0
Temperature at discharge turbine inlet	411.5
Temperature downstream intercooler	20.0
Temperature difference at recuperator hot end	8.0
External fuel delivery temperature	15.0
Fuel gas preheating temperature	120.0
Cooling water temperature	15.0
Limitation on cooling water outlet temperature	25.0

Pressure assumptions (all in bar)	
Ambient pressure	1.013
External fuel delivery pressure	32.000
Cooling water pressure	2.000
Pressure ratio assumptions	
Pressure ratio of charger compressor (total)	6.00
Pressure ratio of LP charger compressor	2.54
Pressure ratio of main compressor (total)	9.80
Pressure ratio of LP main compressor	3.15
Relative pressure drop assumptions (all in %)	
Pressure drop in the charger compressor inlet	1.0
Pressure drop in the after-cooler	3.0
Pressure drop in the recuperator up flow (HP) [8]	5.0
Pressure drop in the recuperator down flow (LP)[9]	3.0
Pressure drop in intercooler	3.0
Pressure drop in the combustor	4.0
Pressure drop in the charger turbine exhaust system	4.0
Pressure drop in the fuel system	10.0
Cooling water pressure drop through heat exchangers	2.5
General cycle data assumptions	
Air humidity (%)	60
Oxygen excess factor in combustor	1.12
Fuel LHV (kJ/kg)	50015
Recirculation ratio (%)	67.5
Cooling air ratio for main turbine (%)	7.0

[8] The recuperator is composed of three heat exchangers. The pressure drop in each exchanger is the third part of the total pressure drop indicated in the table.

[9] The same as the indicated in footnote 7 is considered here.

7 Process simulation of the CCGT plant

7.1 Simulation software

The aim of the simulation process of this thesis is to develop a reference combined cycle gas turbine case and a semi-closed recuperated cycle in order to compare them. Subsequently, a sensitivity analysis of the SCRC is made with the aim of knowing the impact that variations in a certain parameter have on the model.

EBSILON®Professional (version 10.06) is the software used for the simulations commented above. This software permits to simulate thermodynamic cycle processes and is used for engineering, designing and optimizing plants (STEAG Energy Services GmbH).

7.2 Results

A scheme of the combined cycle plant designed, and the results displayed by EBSILON are shown in Figure 7.1.

Studying the different outputs in the steam cycle, it can be concluded that most of the fluid goes through the HP path of the HRSG (91 kg/s), and only a modest load becomes LP steam (27 kg/s). Thus, more heat is exchanged in the HP part of the HRSG. The reason for using a dual-pressure HRSG are first to decrease the temperature of the flue gas stack, which has to be minor than 100 ºC, and second to extract more heat from the flue gas. Using one-pressure level HRSG, the temperature is over this number, and therefore the difference between the gas discharged temperature and the ambient temperature is increased.

The steam quality (x=0.88) at the exit of the turbine is a restrictive parameter of the cycle. To maintain at least 87 % of the quality (x=0.87) at the turbine exit is indispensable to avoid erosion in turbine blades. Therefore, if the quality of the mixture passing through the turbine becomes lower, the impact of the liquid droplets of the liquid-steam mixture can erode the turbine blades. This leads to a decrease of the turbine efficiency, and an increase of the need for maintenance (Moran and Shapiro, 2006).

The exhaust gas composition is a relevant output in order to know if greenhouse gas emission limits in places for electricity generation are accomplished. This result can also be useful for comparing the plant designed with other cycles in terms of pollution. This will be commented after obtaining the rest of the results.

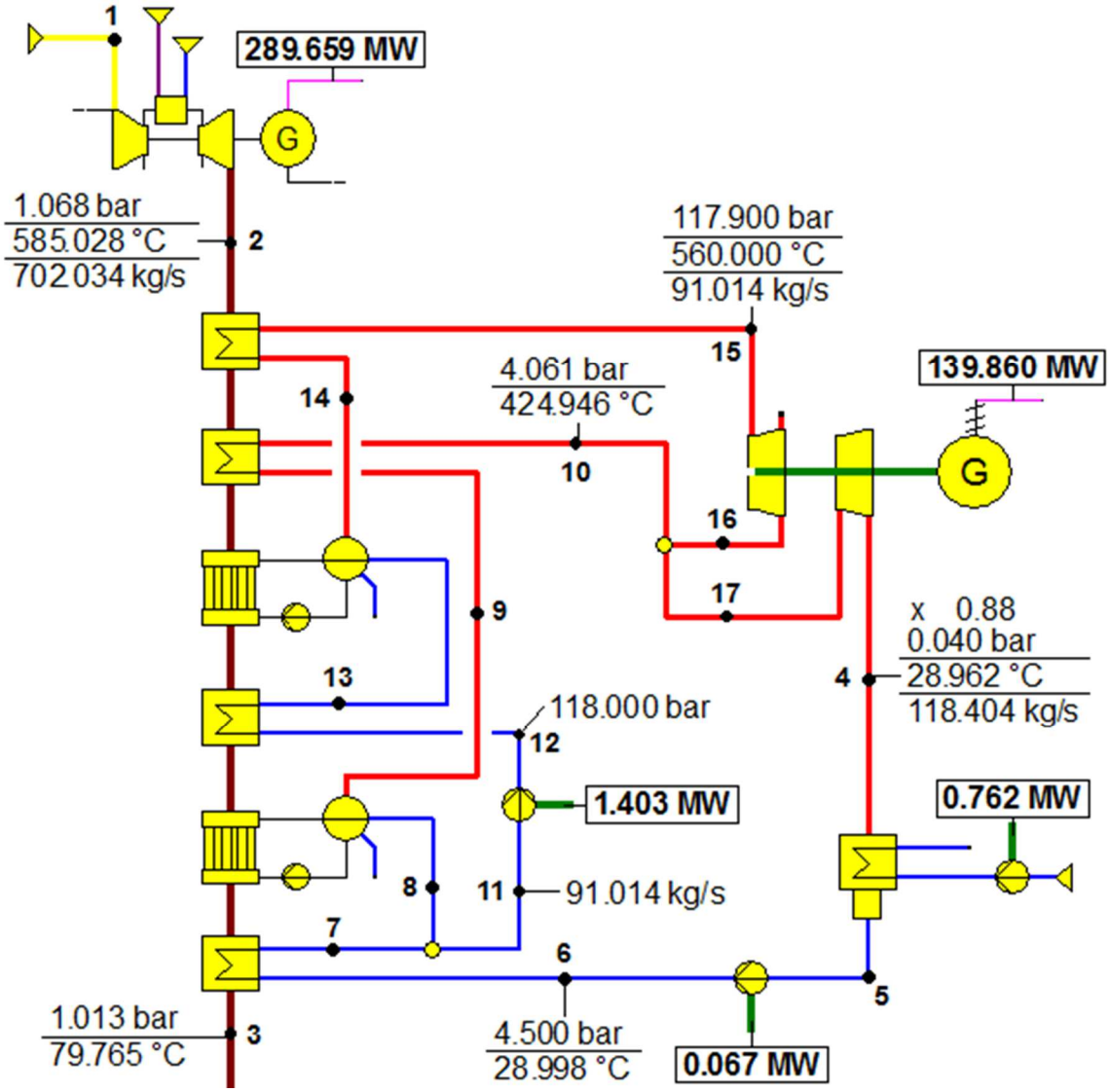

Figure 7.1 Results of the CCGT designed. Relevant outputs not marked in the scheme: air inlet (1) at ISO conditions flow = 687 kg/s; fuel flow (15 ºC, 32 bar) = 15 kg/s; net power output = 427 MW; $\mathbf{Q_{HRSG}}$ = 395 MW; $\mathbf{Q_{condenser}}$ = 254 MW; flue gas composition (mole %): N_2 = 74.51, O_2 = 12.42, Ar = 0.89, H_2O = 8.43, CO_2 = 3.75 (0.0582 $kg_{CO2}/kg_{FLUE\ GAS}$).

Using the data displayed by EBSILON, the efficiency (η) is later calculated as follows:

$$\eta\ (\%) = \frac{W_{net,plant}}{\dot{m}_{fuel} \cdot LHV} \cdot 100 \qquad \text{(Equation 7.1)}$$

where $W_{net,plant}$ is the net power developed by the plant in kW

$\dot{m}_{fuel}$ represents the fuel consumption in kg/s

LHV is the lower heating value of the fuel in kJ/kg

Equation 7.2 represents the specific power related to the air inlet flow rate (SP).

$$\text{SP (kJ/kg air)} = \frac{W_{net,plant}}{\dot{m}_{air}} \qquad \text{(Equation 7.2)}$$

where $W_{net,plant}$ is the net power of the plant in kW

$\dot{m}_{air}$ is the air mass flow rate in kg/s

The specific CO_2 flow rate in the flue gas related to the power output (CO2R) is:

$$\text{CO2R (kg/kWh)} = \frac{\dot{m}_{out,\,GT} \cdot x_{CO_2}}{W_{net,plant}} \cdot 3600 \qquad \text{(Equation 7.3)}$$

where $\dot{m}_{out,\,GT}$ is the mass flow after the gas turbine in kg/s

x_{CO_2} is the CO_2 mass concentration in the flue gas

$W_{net,plant}$ is the net power of the plant in kW

The heat exchange in HRSG or condenser is given in Equation 7.4.

$$\text{Heat exchange in HRSG/condenser (\%)} = \frac{Q_i}{W_{net,plant}} \cdot 100 \qquad \text{(Equation 7.4)}$$

where Q_i is the heat power exchanged in the HRSG/condenser in kW

$W_{net,plant}$ is the net power developed by the plant in kW

The results after applying these formulas are compiled in Table 7.1. The table reveals that the net efficiency of the cycle designed is tolerable, and it is at the same level as combined cycle plants in operation.

Table 7.1 Properties of the CCGT calculated

Plant net power (MW)	427
Plant net efficiency (%)	57.7
Specific power related to the air inlet flow rate (kJ/kg)	622
Specific CO_2 flow rate in flue gas related to the power output (kg/kWh)	0.344
Heat exchange in HRSG related to power output (%)	92.4
Heat exchange in condenser related to power output (%)	59.3

The heat requirement is noticeably higher in the heat recovery steam generator than in the condenser. This means that most of the heat exchange takes place in the HRSG. Accordingly, the HRSG is an important device to pay attention to when designing the CCGT.

Concerning the specific CO_2 flow rate contained in the flue gas related to the power output, the value obtained should not be preferably over 450 g/kWh (Llywodraeth Cymru Welsh Government, 2014). This limit value takes into consideration proposed carbon pollution standards. United States Environmental Protection Agency (EPA) proposed an emission limit for CO_2 at 1000 lb/MWh for larger electric utility generating units (United States Environmental Protection Agency, 2014). In this simulation, it takes a value of 344 g/kWh. Thus, it represents acceptable emissions of CO_2.

When using natural gas as a fuel, another greenhouse and pollutant gases such as NO_x are liberated during the combustion. Methane escapes to atmosphere can also occur. Nevertheless, the model proposed does not contemplate these emissions.

Last but not less important, some representative diagrams of the cycle are presented. T-q diagram for the dual-pressure heat system is displayed in Figure 7.2. The diagram is precisely linked with the chosen pressures at which the steam is raised. In case the pressures were different, the HRSG would work in a different manner and the diagram would be considerably changed.

As expected, the temperature remains constant during evaporations. The LP steam boils at a lower temperature than the HP steam, and therefore two different pinch points between the exhaust gas and the saturated steam temperatures can be situated in the graphic. Additionally, exploring Table 7.2 and Figure 7.2, it can be affirmed that most of the heat exchange takes place in the HP path of the HRSG.

Table 7.2 Table of results for the HRSG

Cold end temperature difference (K)	50.8
Hot end temperature difference (K)	25.0
HP pinch point temperature difference (K)	10.0
LP pinch point temperature difference (K)	10.0
LP economizer thermal power (MW)	57
HP economizer thermal power (MW)	78
LP evaporator thermal power (MW)	59
HP evaporator thermal power (MW)	112
LP superheater thermal power (MW)	16
HP superheater thermal power (MW)	75

Considering only one part of the HRSG (HP or LP) and by comparing the thermal powers in evaporator, superheater and economizer of this part, one can deduce that the evaporator is the device where most of the heat is exchanged.

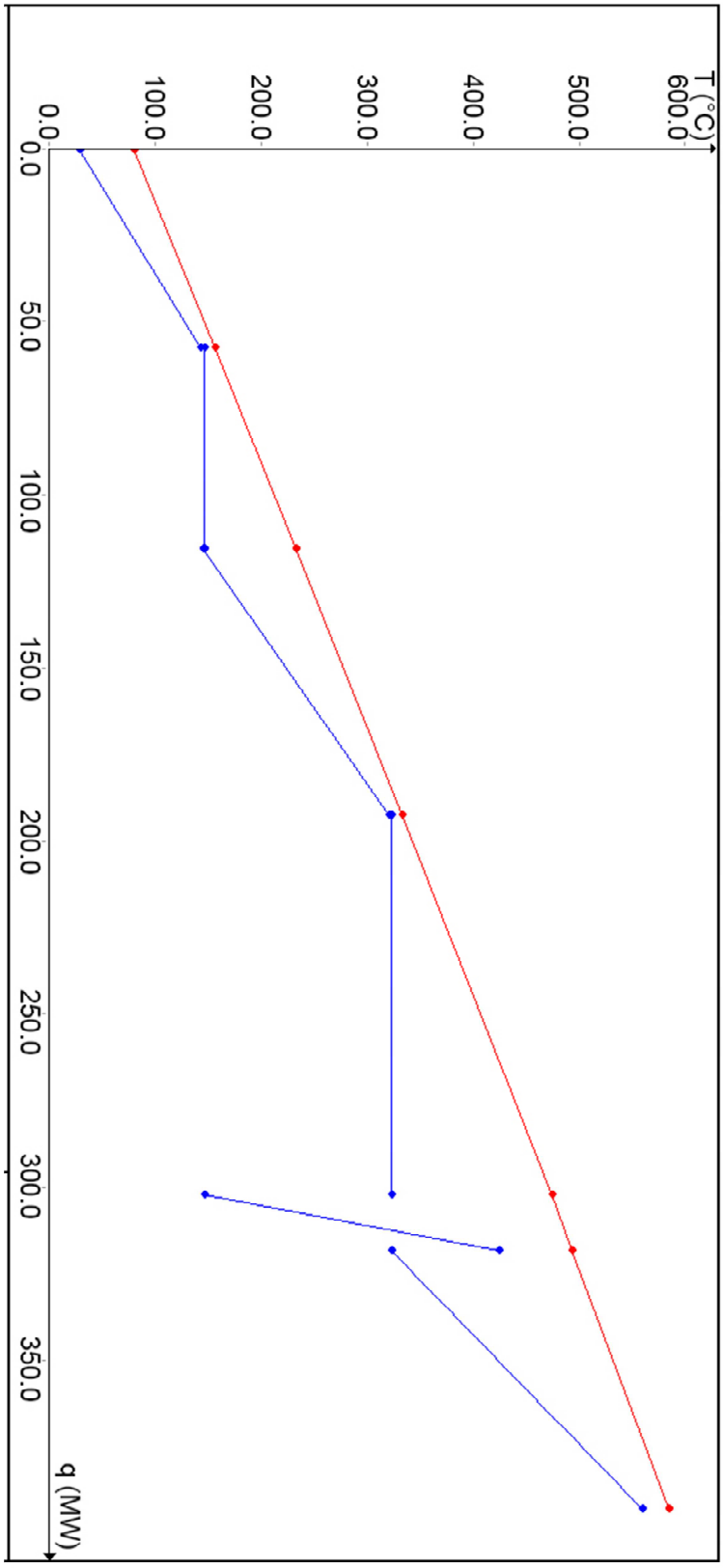

Figure 7.2 TQ diagram for the dual-pressure reheat HRSG. Red lines refer to HRSG flue gas, and blue lines to water/steam cycle. The steepest slop corresponding to the LP superheater is due to the fairly amount of steam going through the device and the situation of the superheater. Hence it is easier to warm up.

In Figure 7.3 the temperature – specific entropy diagram for the dual-pressure combined cycle is plotted. It is relevant to comment that the diagram presented does not consider the gas turbine cycle.

The complete cycle is included in Appendix. The GT cycle shown is an approximation due to the fact that the diagrams for the gas turbine chosen in the VTU Library are not available in the software.

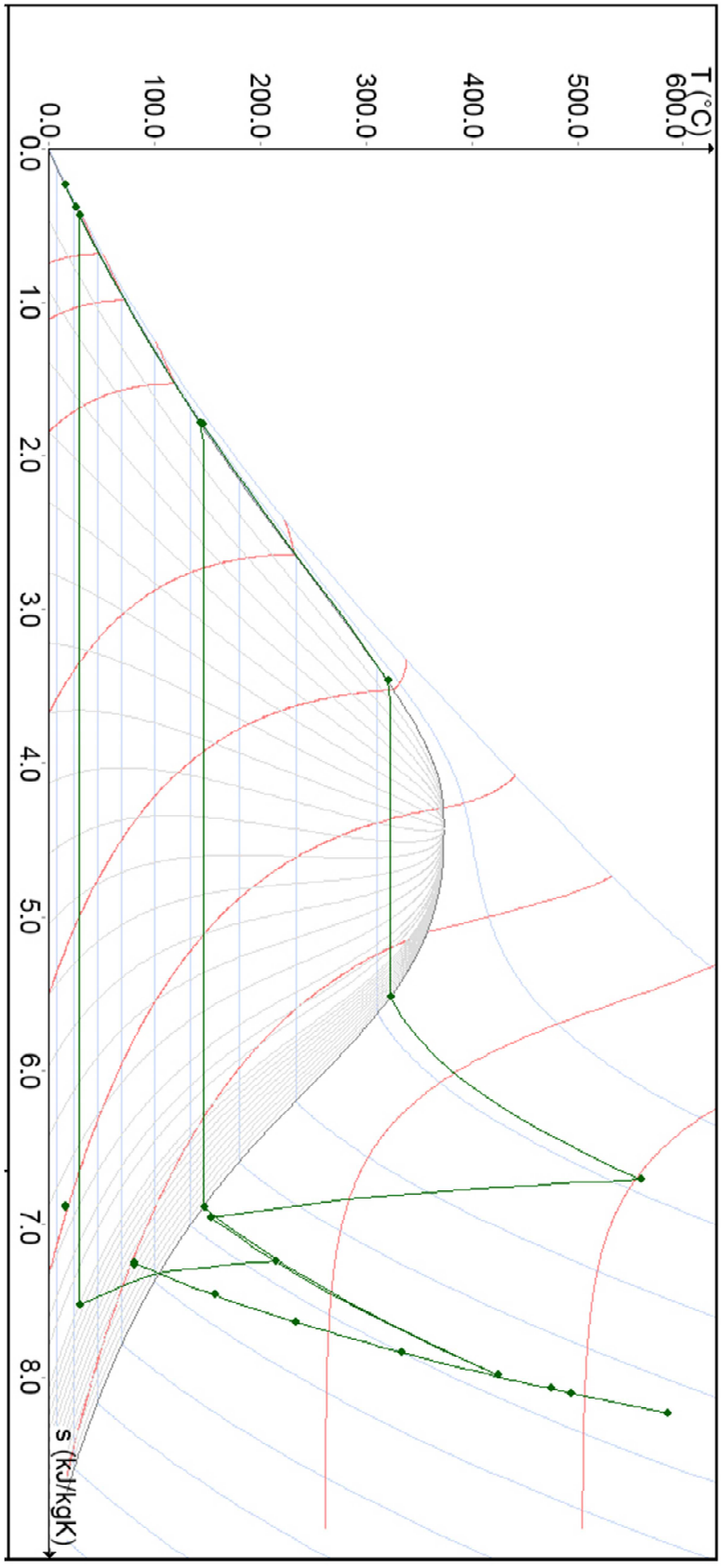

Figure 7.3 Temperature – specific entropy diagram of the CCGT designed

7.3 Validation of the reference case

The results of the simulated cycle are comparable to existing and operating combined cycles, for instance San Severo combined cycle plant. This plant produces roughly the same electricity as the simulated one, and it uses the same model of turbine, which is an important characteristic for the validation of the model.

San Severo 1 x 400 MW combined cycle plant (Ansaldo Energia) is situated in Italy. The plant reaches over 57 % of efficiency. The plant is composed of a 1+1 combined cycle unit. The unit consists of one AE94.3A gas turbine, one MT15 steam turbine, and a 50THR generator. The configuration of these components is in single shaft with air condenser as cooling system. The main fuel of the gas turbine AE94.3A x 280 MW-50 Hz is natural gas. The steam turbine produces 135 MW at base load (50 Hz). The steam is raised at three different pressures: 118.00, 30.30 and 4.63 bar. The heat recovery steam generator has three pressure levels, natural circulation and a drum type with integrated daerator.

Figure 7.4 San Severo combined cycle plant (Ansaldo Energia)

The data available for the plant is limited. However, the simulation were made on the basis of literature sources with realistic assumptions. Hence, the outputs obtained with EBSILON were the ones expected, and they agree with the typical values of a common combined cycle gas turbine.

The discrepancies that appear are expected since firstly the assumptions for our model are most likely not corresponding to the real plant. The design of the HRSG is also different. As it has an important impact into the cycle, discrepancies are perfectly expected. Moreover, a certain overall incertitude in the calculations and the software is always present.

After analyzing our model and the real plant as far as possible, it is concluded that the plant simulated could be considered reliable and it offers acceptable output results.

8 Process simulation of the SCRC plant

8.1 Simulation

As in the reference case, the simulation has been run with the software EBSILON®professional (version 10.2). As commented in Chapter 6, two different alternatives of the semi-closed recuperated cycle are simulated:

- Variant 1: semi-closed recuperated cycle with one intercooler in the pressurized group.
- Variant 2: semi-closed recuperated cycle with intercooling after each low-pressure compressor.

8.2 Results of variant 1

For the semi-closed recuperated cycle with intercooling in the main loop, the results are not explained because of their similarity with the outputs of the SCRC with two intercoolers.

For having a global vision of the plant, the most relevant results are shown visually in Figure 8.1. For comprehending the thermodynamic cycle, the temperature – specific entropy graphic is pointed out in Figure 8.2. The graphic TQ for the recuperator is the same as the one shown in Figure 8.7. Moreover, Table 8.2 includes the rest of the outputs and data calculated using the same equations applied for the other variant. The complete stream table is included in Appendix.

Like in the other case, the heat that could be extracted from the exit cooling water of the after-cooler is calculated. This fluid contains energy enough (80 MW) in order to cover the energy necessary for preheating the cooling fluid (2 MW).

Table 8.1 Cooling water temperatures in after-cooler and intercooler of variant 1

Cooling water temperatures (all in ºC)	In	Out
After-cooler water temperature	15.0	32.6
Intercooler water temperature (main group)	15.0	24.4

$$\dot{Q}_{w,after-cooler} = \dot{m}_{cw} C_p \Delta T = 2500.0\ {}^{kg}/_{s} \cdot 4.2\ {}^{kJ}/_{kgK} \cdot (32.6 - 25.0)K = 79\,800\ kW$$

Not all the energy that could be extracted from the cooling fluid is used for preheating. There is a possibility to increase the water rate in order to not loss energy, and accomplishing the limitations in water cooling.

Table 8.2 Results of the SCRC with intercooling in the main loop

Net power (MW)	421
Recuperator thermal power (MW)	711
After-cooler thermal power (MW)	184
Main turbine thermodynamic power (MW)	617
Main compressor thermodynamic power (MW)	193
Charger compressor thermodynamic power (MW)	58
Discharge turbine thermodynamic power (MW)	64
Fuel gas compressor power (MW)	2
Combustor thermal power (MW)	716
Main group intercooler heat discharge (MW)	99
Power necessary for preheating the fuel (MW)	2
Condensed water flow rate in after-cooler (kg/s)	21.9
Condensed water in charger group intercooler (kg/s)	0.0
Condensed water in main group intercooler (kg/s)	1.3
Totally condensed water flow rate (kg/s)	23.2
Methane fuel flow rate (kg/s)	14.3
Main turbine exit flow rate (kg/s)	791.2
Hot gas density at main turbine inlet (kg/m^3)	9.9
Data calculated	
Plant net efficiency (%)	58.8
Specific power related to the air inlet flow rate (kJ/kg)	1583
Specific CO_2 flow rate in discharge related to the power output (kg/kWh)	0.337
Heat exchange in recuperator related to power output (%)	169.0
Heat exchange in after-cooler related to power output (%)	43.6
Heat exchange in main group intercooler related to power output (%)	23.4

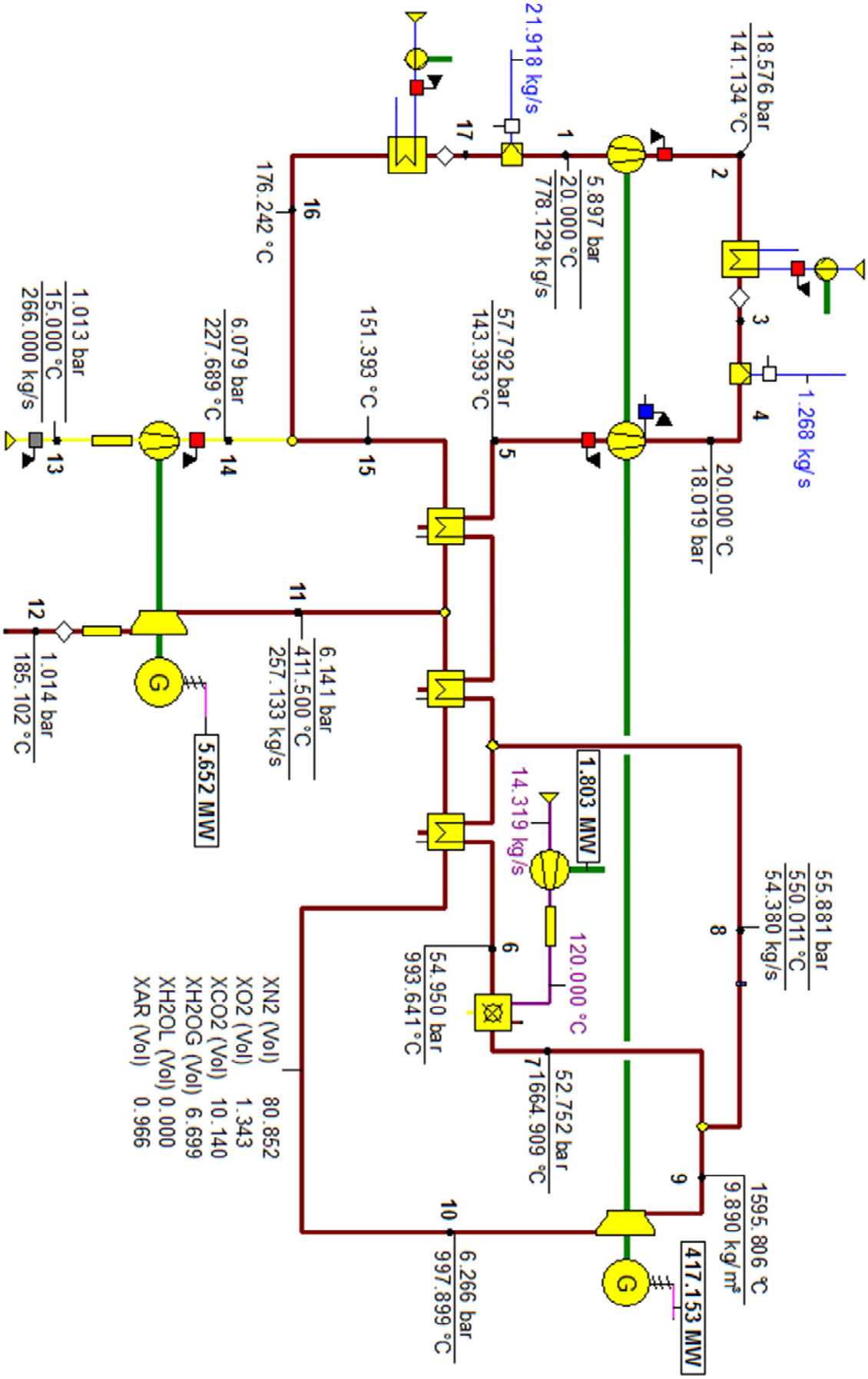

Figure 8.1 Results of the SCRC with intercooling in the main group

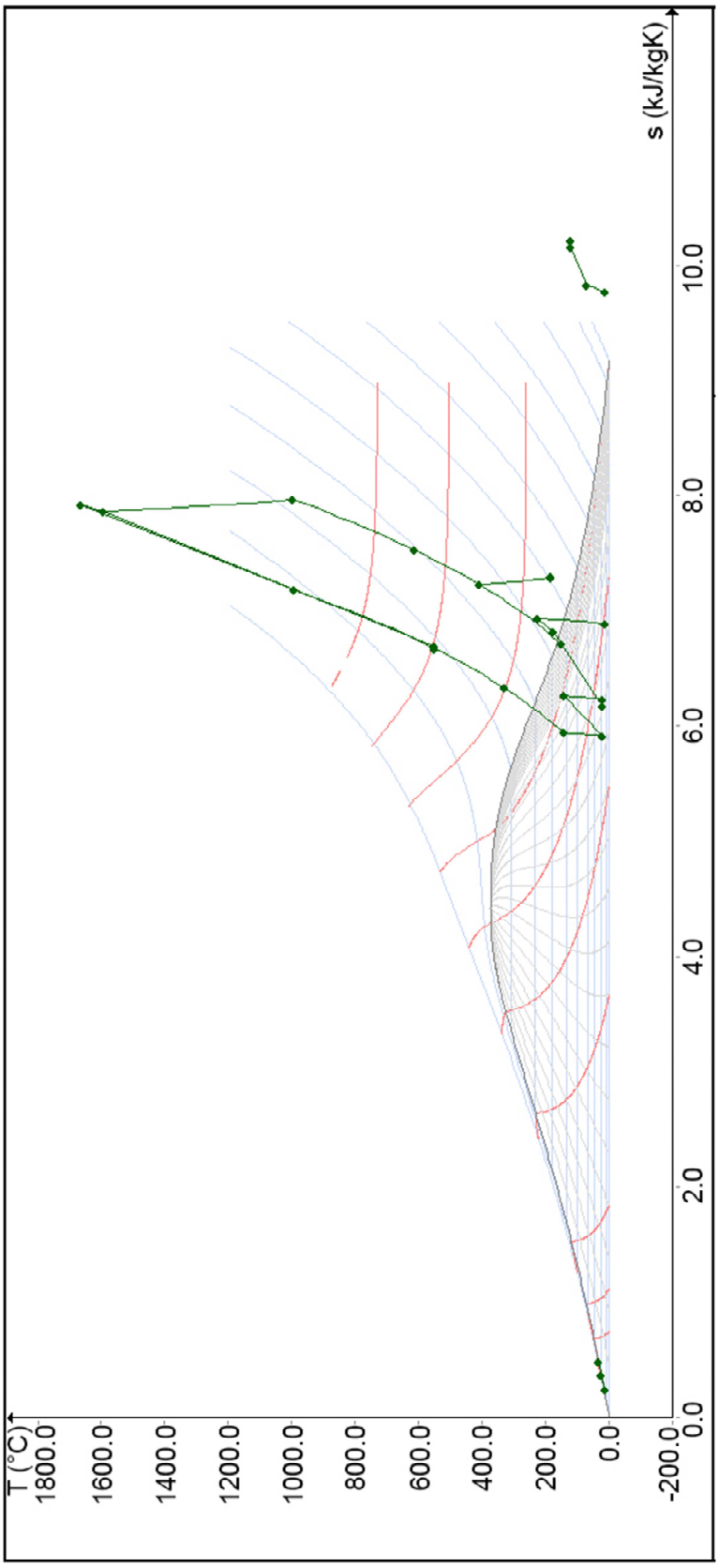

Figure 8.2 Temperature – specific entropy graphic of the variant with one intercooler in the main loop

8.3 Results of variant 2

The following stream table gives information about pressures, temperatures, mass flows, and compositions for each of the points studied in SCRC.

Table 8.3 Stream table of the second variant. Numbering in accordance with Figure 6.4 in Chapter 6. Composition of the gas is important to follow because of its changes. For streams 3, 17 and 19, the composition percentage does not take into consideration the water extracted. Therefore the total is not 100%.

Stream nr	P (bar)	T (ºC)	m (kg/s)	Composition (mole %)					
				Ar	N_2	O_2	CO_2	H_2O (g)	H_2O (l)
1	5.897	20.0	778	0.996	83.376	8.164	7.068	0.397	0.000
2	18.576	141.1	778	0.996	83.376	8.164	7.068	0.397	0.000
3	18.019	20.0	778	0.996	83.376	8.164	7.068	0.129	0.003
4	18.019	20.0	777	0.999	83.600	8.185	7.087	0.130	0.000
5	57.792	143.4	777	0.999	83.600	8.185	7.087	0.130	0.000
6	54.95	993.6	722	0.999	83.600	8.185	7.087	0.130	0.000
7	52.752	1664.9	737	0.963	80.652	0.846	10.362	7.176	0.000
8	55.881	550.0	54	0.999	83.600	8.185	7.087	0.130	0.000
9	52.752	1595.8	791	0.966	80.852	1.343	10.140	6.699	0.000
10	6.266	997.9	791	0.966	80.852	1.343	10.140	6.699	0.000
11	6.141	411.5	257	0.966	80.852	1.343	10.140	6.699	0.000
12	1.014	185.1	257	0.966	80.852	1.343	10.140	6.699	0.000
13	1.013	15.0	266	0.924	77.393	20.646	0.026	1.010	0.000
14	6.079	113.8	266	0.925	77.450	20.661	0.026	0.937	0.000
15	6.079	151.4	534	0.966	80.852	1.343	10.140	6.699	0.000
16	6.079	139.2	800	0.952	79.714	7.805	6.757	4.772	0.000
17	5.897	20.0	800	0.952	79.714	7.805	6.757	0.379	0.044
18	2.574	113.4	266	0.924	77.393	20.646	0.026	1.010	0.000
19	2.496	20.0	266	0.924	77.393	20.646	0.026	0.936	0.001
20	2.496	20.0	266	0.925	77.450	20.661	0.026	0.937	0.000

As it can be appreciated in Table 8.3, the composition of the gas presents a wide range of values with considerable changes. This occurs due to several reasons: the water extraction after intercoolers and after-cooler, the recirculation of the most part of the flue gas, and the mix of the cooling fluid into the exhaust gas after the combustor.

Starting at stream number 1, which corresponds to the main LP compressor inlet flow, it can be appreciated that the fluid compressed has a considerably lower content of oxygen (O_2), and higher carbon dioxide (CO_2) and water (H_2O) concentrations compared to ISO air composition (stream 13). As expected, the composition remains constant until the condensed water in the intercooler is extracted (stream 4). Through the recuperator (HP and LP paths) the composition is also conserved. The most important change in composition is when it is combined with fuel, and combustion takes place. The contents of CO_2 and H_2O in stream 7 are considerably higher because of the combustion reaction, which liberates the mentioned components. On the other

hand, very low values of O_2 are detected. After the cooling fluid mixing point (stream 9) the composition is again altered, but the changes are not so pronounced. This cycle produces a near stoichiometric composition in the discharged fluid (stream 11), and its CO_2 fraction represents 10.14 % by mole of the exhaust flow. For this reason the SCRC is characteristically carbon capture and storage (CCS) ready.

Concerning mass flows, most part of the flue gas is recirculated and only meager part of the flue gas is led to the discharge turbine (257 kg/s), which is slightly lower than the air introduced into the pressurized loop (266 kg/s) but with more energy. Mass flows through turbomachinery in the main loop are around 700-800 kg/s.

In order to understand variations in temperatures and pressures, different diagrams are presented below using the values indicated in Table 8.3, and their corresponding specific volume data. Each point of the thermodynamic cycle is shown with its matching stream number (see Figure 6.4 in Chapter 6). The description of each process is explained under each graphic for better understanding. In all charts the semi-closed loop is easy to recognise, as well as the charger group.

The first chart reveals the temperature versus specific volume graphic, whereas the relation between pressure and specific volume is illustrated in the second one. There are not isothermal, isochoric, or isobaric processes, apart from mixing and splitting (where P and T are constants).

The first chart (Figure 8.3) shows that the temperature after combustor (7) presents the highest value as expected. This high value justifies the cooling fluid (8) use, which permits to reduce the TIT approaching 1600 ºC (9). The amount of cooling fluid and the temperature at which it is discharged could be useful to regulate the main TIT. The excess fluid point could also be discharged at different temperature, and it is helpful to choose the desired discharger TIT.

Regarding Figure 8.4, it can be comprehended that the main group turbomachinery works at considerably high pressures, and this will be crucial when designing the different devices. Variances in pressures are due to pressure drops considered in the machinery, and obviously due to the existence of compressors and turbines.

When pressures reached by the charger and the main compressors are compared, it can be noticed that the pressure reached by the main group is reasonably higher (57.8 bar). If needed, this pressure could be increased or decreased by changing the values of compressors' pressure ratios, affecting probably the efficiency of the cycle.

The same occurs if pressure differences before and after main and discharge turbines are contrasted. Therefore, the power output provided by the main turbine is considerably higher than the power output of the discharge turbine.

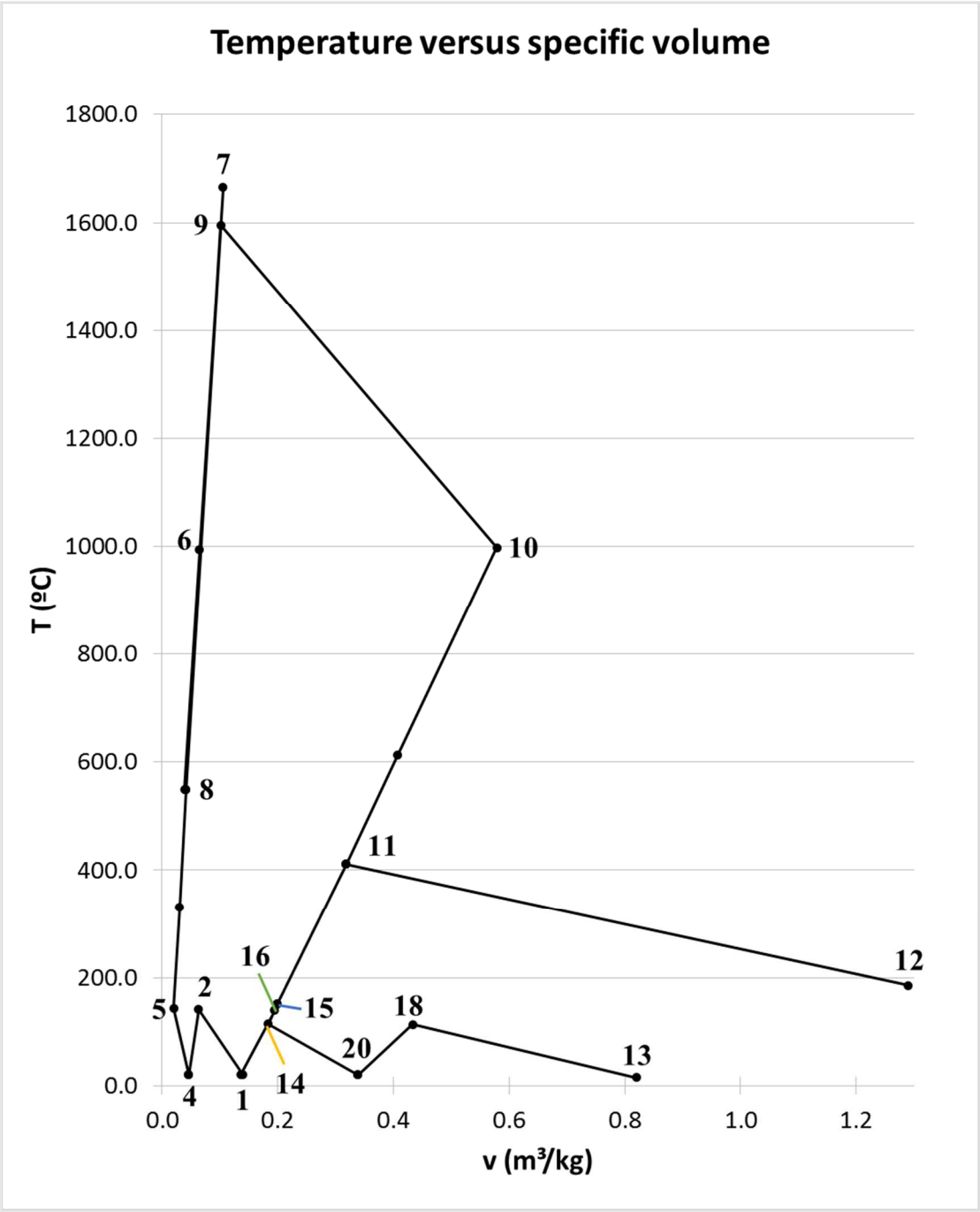

Figure 8.3 Temperature – specific volume diagram of the second variant. Processes**:** (13→18) air compression in LP charger compressor; (18→20) intercooling; (20→14) compression in HP charger compressor; (14→16) mixing compressed air into recirculated gas; (16→1) mixture after-cooling; (1→2) mixture compression in LP main compressor; (2→4) intercooling; (4→5) mixture compression in HP main compressor; (5→6) mixture compressed heating up in HP path of recuperator; (6→7) combustion; (7→9) mixing cooling fluid into flue gas; (9→10) flue gas expansion in main turbine; (10→15) flue gas cooling down in LP path of recuperator; (11→12) discharged flue gas expansion in discharge turbine.

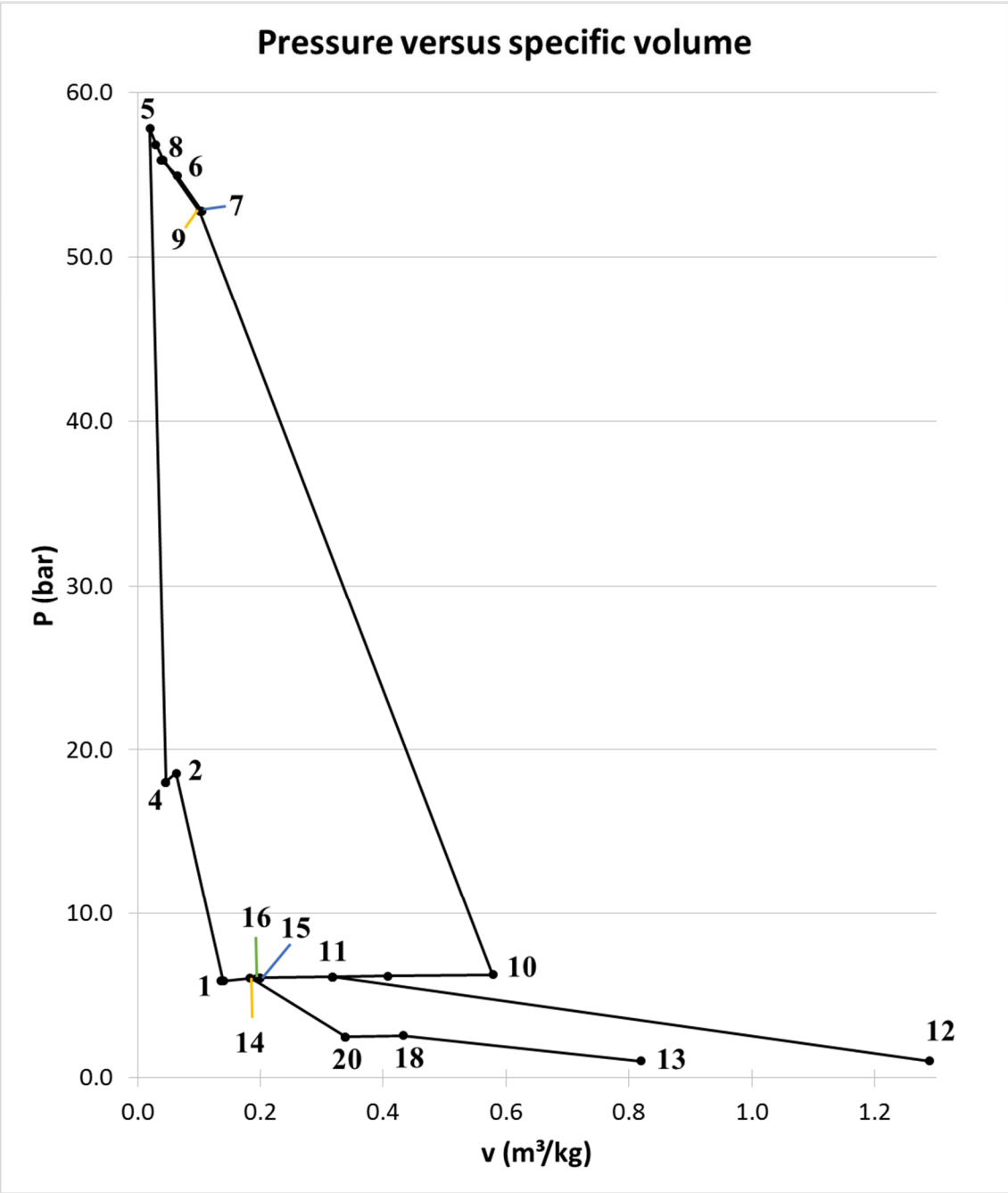

Figure 8.4 Pressure – specific volume diagram of the second variant. Processes: (13→18) air compression in LP charger compressor; (18→20) intercooling; (20→14) compression in HP charger compressor; (14→16) mixing compressed air into recirculated gas; (16→1) mixture after-cooling; (1→2) mixture compression in LP main compressor; (2→4) intercooling; (4→5) mixture compression in HP main compressor; (5→6) mixture compressed heating up in HP path of recuperator; (6→7) combustion; (7→9) mixing cooling fluid into flue gas; (9→10) flue gas expansion in main turbine; (10→15) flue gas cooling down in LP path of recuperator; (11→12) discharged flue gas expansion in discharge turbine.

The temperature – specific entropy diagram is given in Figure 8.6. It helps overviewing the thermodynamics of the cycle studied. The diagram shows the same tendency as the one found in literature (Wettstein, 2014b), which is presented in Figure 8.5.

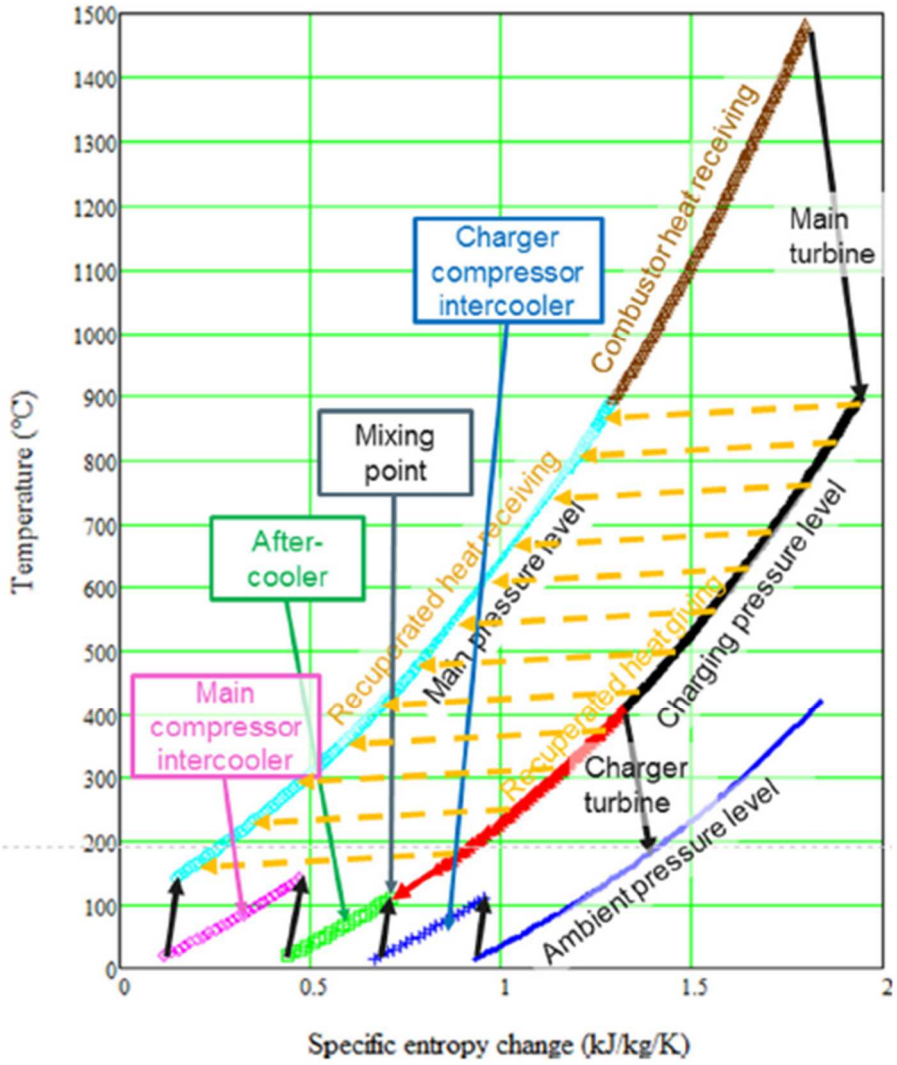

Figure 8.5 Temperature – specific entropy diagram of an intercooled SCRC (Wettstein, 2014b)

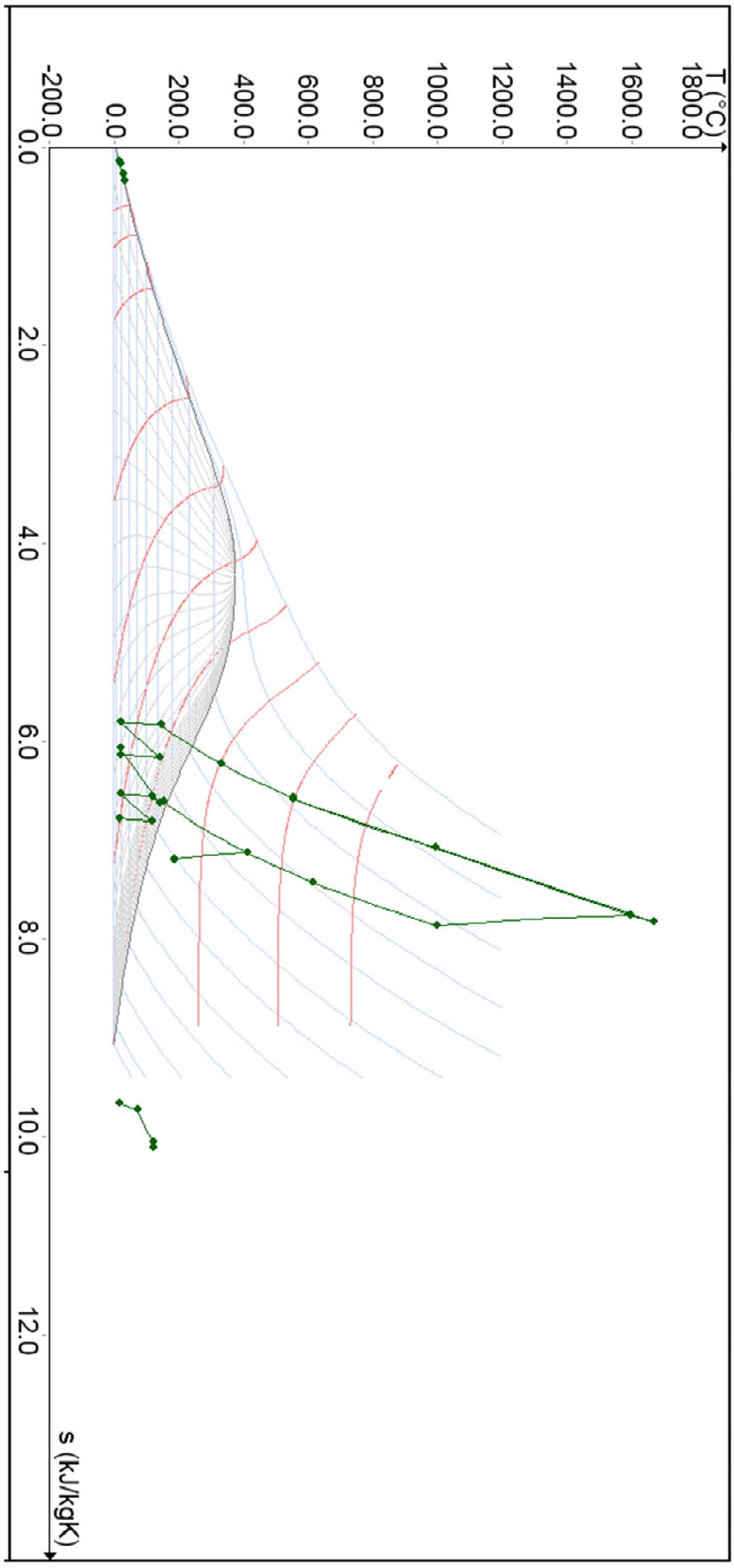

Figure 8.6 Temperature – specific entropy diagram of the second variant

The rest of the data for variant 2 are presented in Table 8.4.

Water is condensed and extracted from the gas, which means that this cycle produces water. This water could be profitable, especially when the plant is situated in arid zones and an air cooling system is applied.

One of the important characteristics of the cycle is the density of the gas at main turbine inlet. As shown in table, this value is high, which permits that more mass flow can go through the turbomachinery and therefore, more power output can be produced. Without using so much fuel and introducing 266 kg/s of air, it is possible to produce electric power around 420 MW.

Table 8.4 Results of the second variant

Net power (MW)	427
Recuperator thermal power (MW)	711
After-cooler thermal power (MW)	152
Main turbine thermodynamic power (MW)	617
Main compressor thermodynamic power (MW)	193
Charger compressor thermodynamic power (MW)	52
Discharge turbine thermodynamic power (MW)	64
Fuel gas compressor power (MW)	2
Combustor thermal power (MW)	716
Main group intercooler heat discharge (MW)	99
Charger group intercooler heat discharge (MW)	25
Power necessary for preheating the fuel (MW)	2
Condensed water flow rate in after-cooler (kg/s)	21.8
Condensed water in charger group intercooler (kg/s)	0.1
Condensed water in main group intercooler (kg/s)	1.3
Totally condensed water flow rate (kg/s)	23.2
Methane fuel flow rate (kg/s)	14.3
Main turbine exit flow rate (kg/s)	791.2
Hot gas density at main turbine inlet (kg/m^3)	9.9

As we move ahead, different important outcomes are calculated with the numbers presented in this table.

The most important value is the net efficiency of the plant. As it was commented in Chapter 6, the efficiency is calculated as the net power produced by the plant divided by the fuel consumption and its LHV. Cooling water pumps power are not considered because their power required are negligible compared to the power output. Another important thing that affects efficiency calculation is if there is enough energy in the cycle in order to preheat the fuel until 120 ºC. If this energy extracted is not enough, the efficiency of the plant should be calculated taking into consideration the heat necessary to preheat it. Table 8.5 is used for corroborating that the energy can be extracted from the energy contained in the cooling water.

Table 8.5 Cooling water temperatures in after-cooler and intercoolers

Cooling water temperatures (all in ºC)	In	Out
After-cooler water temperature	15.0	29.6
Intercooler water temperature (charger group)	15.0	17.4
Intercooler water temperature (main group)	15.0	24.4

Due to environmental reasons, the cooling water outlet temperature was limited at 25 ºC. Examining the table, the after-cooler's water outlet temperature excess this limit, and the energy that could be extracted is approximately 48 MW

$$Q_{w,after-cooler} = \dot{m}_{cw} C_p \Delta T = 2500.0\ {}^{kg}/_{s} \cdot 4.2\ {}^{kJ}/_{kgK} \cdot (29.6 - 25.0)K = 48\,300\ kW$$

Hence, it is demonstrated that there is enough energy that could be extracted from the cooling fluid in order to cover the 2 MW necessary for preheating. Therefore, the equation for calculating the net efficiency is valid.

In case that this energy would not have been enough, the heat of the gas after the discharge turbine could be used to increase the fuel temperature to 120 ºC.

Another output is the specific power (SP) related to the air inlet flow rate. It is calculated as follows:

$$SP\ (kJ/kg\ air) = \frac{W_{net,plant}}{\dot{m}_{air}} \qquad \text{(Equation 8.1)}$$

where $W_{net,plant}$ is the net power of the plant in kW

$\dot{m}_{air}$ is the air mass flow rate in kg/s

The specific CO_2 flow rate in discharge related to the power output is (CO2R):

$$CO2R\ (kg/kWh) = \frac{\dot{m}_{out,\,GT} \cdot (1\text{-}RR) \cdot x_{CO_2}}{W_{net,plant}} \cdot 3600 \qquad \text{(Equation 8.2)}$$

where $\dot{m}_{out,\,MT}$ is the mass flow after the main turbine in kg/s

RR is the recirculation ratio

x_{CO_2} is the CO_2 mass concentration in the discharged fluid

$W_{net,plant}$ is the net power of the plant in kW

Finally, the heat exchange in recuperator/after-cooler/intercooler is given by $Q_i/W_{net,plant}$ where Q_i is the heat power exchanged in the recuperator/after-cooler/intercooler in kW, and $W_{net,plant}$ is the net power developed by the plant in kW.

The results are shown in Table 8.6. From the presented data, it can be appreciated that the plant offers a high efficiency. The specific power would be useful when comparing with other cycles. The low value of the specific power reduces the size of inlet and outlet ducts.

Table 8.6 Properties of the SCRC calculated

Net efficiency (%)	59.6
Specific power related to the air inlet flow rate (kJ/kg)	1605
Specific CO_2 flow rate in discharge related to the power output (kg/kWh)	0.332
Heat exchange in recuperator related to power output (%)	166.6
Heat exchange in after-cooler related to power output (%)	35.7
Heat exchange in charger group intercooler related to power output (%)	6.0
Heat exchange in main group intercooler related to power output (%)	23.4

The comparison between heats exchanged in the devices presents that the highest value is in the recuperator, followed by the after-cooler, and afterwards the intercoolers. As the recuperator is the device where most heat exchange occurs, it is required more heat exchange area, and therefore its size is substantially higher than the dimension of the intercoolers and after-cooler.

A TQ diagram of the recuperator is plotted in Figure 8.7. It shows the temperature distribution along the length of the heat exchanger, as well as the total heat transferred to the fluid. The recuperator is composed by three different heat exchangers. For this reason each heat exchanger is represented by a different steep line. The cold gas line almost holds the same steep along the recuperator.

The temperatures indicated in Table 8.7 corresponds to the points represented in Figure 8.7. It is worthwhile to comment that the hot end and cold end differences between both gases are very small, what could mean that the heat is better profited.

Depending on how the recuperator is designed, the graphic and temperature differences commented would change.

Table 8.7 Characteristics of the recuperator

Temperature differences in recuperator (all in K)	
at hot end	8.0
at cooling fluid discharge point	63.8
at excess fluid discharge point	80.2
at cold end	4.3

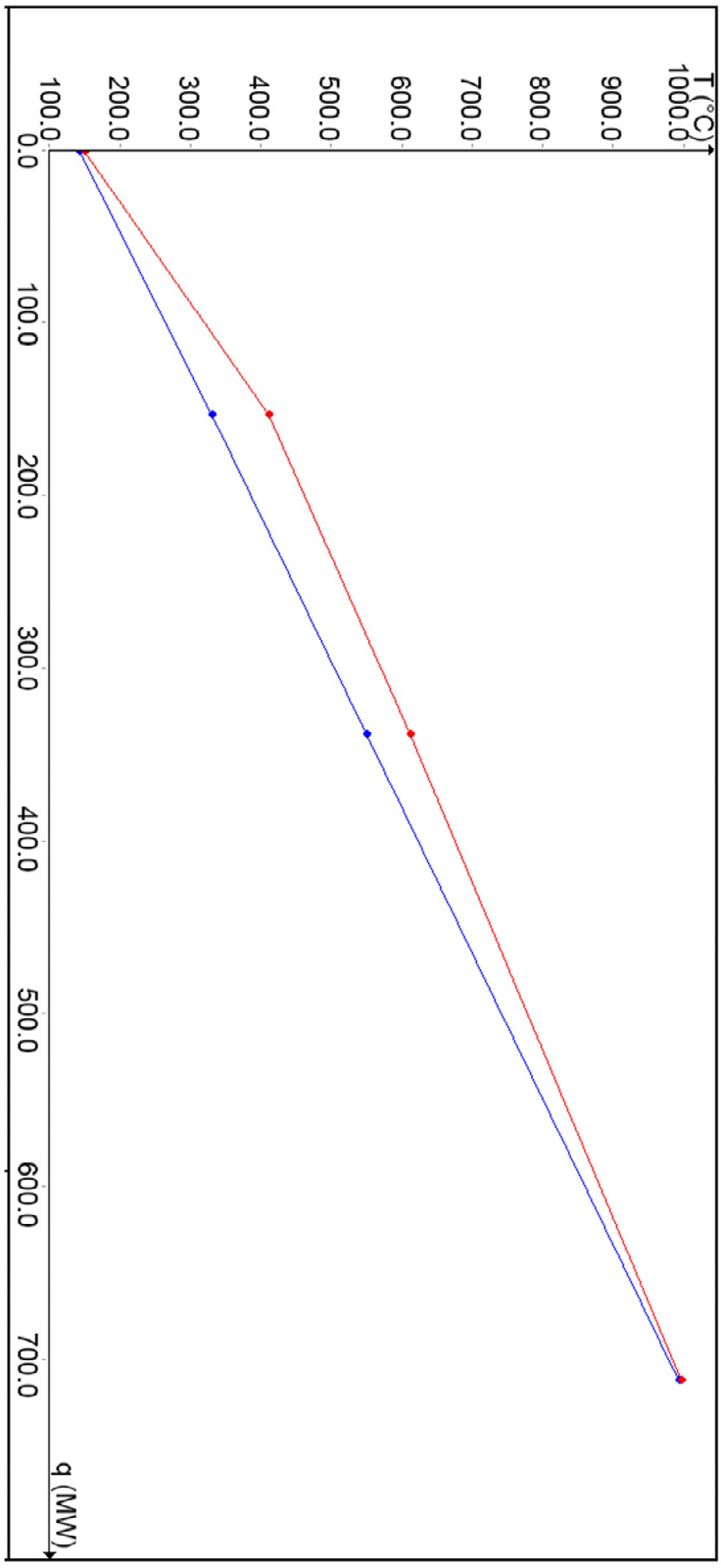

Figure 8.7 TQ diagram of the recuperator of the second variant. Red lines refer to the hot flue gas in the LP path, and blue lines to the cold gas in the HP path. The temperature difference within the recuperator remains higher while two temperature pinch points appear at the hot and cold end of the recuperator.

8.4 Comparison between variants

After analysing the results of the two semi-closed recuperated cycles, it can be concluded that intercooling in both compressors offers a clear advantage with respect to efficiency and power density.

Intercooling in only one of the compressors leads to a higher temperature difference in the mixing point. Therefore, the after-cooler's work increases approximately 22 %, and less water is condensed. The absence of intercooling results in more work for the charger compressor and a decrease in the efficiency (58.8 % in variant 1 and 59.6 % in variant 2).

Moreover, if losses in the mixing point would have been considered, in the first variant the losses would be larger because of a higher difference in temperature in the mixing point. Thus, the efficiency would decrease again.

For its point forward, intercooling in both compressors will be the option to best study due to its potential.

8.5 Validation of the SCRC models

The results of the second variant designed, which considers intercooling in both compressors, are compared to the outcomes of a similar study carried out by Wettstein (2014b). The objective of this comparison is to validate the semi-closed recuperated cycle modelled. The designed model was made on the basis of this literature data, and for this reason it is the best study to compare to.

Most of the input values of the model were chosen reasonably close to the ones used in the study mentioned above. It has to take the assumptions into consideration because not all the assumptions from the designed plant were the same. These different considerations (see Table 8.8) and miscalculations of the software will influence the existing error between the literature data and the results displayed by EBSILON. However, comparing these numbers will give a relevant check according to efficiency, exhaust gas composition, specific power, and heat exchange in recuperator and intercooler related to the power output. The performance of the simulated cycles will be considered valid if the most important results calculated by the program are in within the range of 5% of the outcomes of the study.

Table 8.8 Differences between considerations made in the SCRC model and the literature data

	Variant 2	Wettstein
Type of gas considered	real	ideal
Turbomachinery's efficiencies	isentropic	polytrophic
Cooling fluid mixing point	before turbine	middle turbine
Cooling water temperature (ºC)	15.0	20.0
Temperature after intercooling (ºC)	20.0	25.0
Temperature at cooling fluid discharge from recuperator (ºC)	550.0	500.0
Temperature at discharge turbine inlet (ºC)	411.5	405.6
Cooling air ratio for main turbine (%)	7.0	12.0
Fuel LHV (kJ/kg)	50015	50000

Table 8.9 shows the comparison of the exhaust gas' composition after the main turbine between the model simulated and the data found in literature. The relative error is less than 2.5 %-points for all the elements except for the oxygen, whose error represents approximately 23 %. This is principally due to the cooling fluid recirculation rate, which was an inlet value. It was chosen lower than in the literature case (7 % instead 12 %). This was made in order to obtain a turbine inlet temperature around 1600 ºC. Therefore, the CO_2 concentration is incremented 2.3 %-points.

Table 8.9 Verification table for the flue gas' composition

Fluid composition at main turbine outlet (mass %)	Out of main turbine	
	Simulation	Literature
Argon (Ar)	1.32	1.32
Nitrogen (N_2)	77.74	77.57
Oxygen (O_2)	1.48	1.93
Carbon dioxide (CO_2)	15.32	14.97
Steam (H_2O)	4.14	4.21

In the following table the results from the comparison between the study and simulation data are presented.

Table 8.10 Verification table for the second variant. Relative error data is pointed out in third column. Relative errors higher than 5 % are indicated in red. Most of the results are in the range considered.

	Variant 2	Wettstein	Relative error (%)
Net efficiency (%)	59.6	59.5	0.2
Net power (MW)	427	417	2.3
Recuperator thermal power (MW)	711	615	15.8
After-cooler thermal power (MW)	152	154	1.0
Specific CO_2 flow rate in discharge related to the power output (kg/kWh)	0.332	0.332	0.0
Totally condensed water flow rate (kg/s)	23	22	3.8
Methane fuel flow rate (kg/s)	14	14	2.1
Main turbine exit flow rate (kg/s)	791	793	0.2
Hot gas density at main turbine inlet (kg/m³)	9.9	10.3	4.1
Main turbine thermodynamic power (MW)	617	606	1.7
Main compressor thermodynamic power (MW)	193	192	0.6
Charger compressor thermodynamic power (MW)	52	52	0.5
Discharge turbine thermodynamic power (MW)	64	63	0.6
Fuel gas compressor power (MW)	2	2	0.2
Main group intercooler heat discharge (MW)	99	101	2.2
Charger group intercooler heat discharge (MW)	25	29	13.4
Temperature differences in the recuperator			
.at cooling fluid discharge point (K)	63.8	77.2	17.4
.at excess fluid discharge point (K)	80.2	82.4	2.6
.at cold end (K)	4.3	8.1	47.4
Temperatures in the cycle (all in ºC)			
Recuperator hot end exit temperature	993.6	888.6	11.8
Main turbine inlet temperature	1595.8	1597.8	0.1
Main turbine average exit temperature	997.9	896.6	11.3
Discharge turbine average exit temperature	185.1	181.8	1.8
Charger LP compressor average exit temperature	113.4	113.6	0.2
Charger HP compressor average exit temperature	113.8	113.9	0.1
Main LP compressor average exit temperature	141.1	141.4	0.2
Main HP compressor average exit temperature	143.4	142.6	0.5
Other data			
Specific power related to the external air inlet flow rate (kJ/kg)	1605	1569	2.3
Heat exchange in recuperator related to power output (%)	166.6	147.3	13.1
Heat exchange in after-cooler related to power output (%)	35.7	36.9	3.3
Heat exchange in charger group intercooler related to power output (%)	6.0	7.1	15.3
Heat exchange in main group intercooler related to power output (%)	23.4	24.1	3.1
Combustor thermal power (MW)	716	701	2.1

From the above presented data could be concluded that there is an acceptable match between these values. A major difference appears in recuperator's characteristics principally due to the different design and considerations made for this device.

On the other hand, in variant 2 the cooling gas was mixed with the flue gas from combustor before entering in the main turbine. In Wettstein's study it was mixed when the exhaust gas was going through the main turbine. Therefore, in Table 8.10 can be appreciated a higher error in the average exit temperature.

The heat exchange in the low-pressure intercooler also represents a considerable error. This could be because the cooling water and its flow were considered different (15 ºC and 2500 kg/s respectively).

All the other data are comparable and they have a relative error lower than 5 %. Regardless of these discrepancies commented above, and taking into account their causes, the results are very close to the Wettstein's study, and this fact validates the second model.

For the first case, there is not data available with close assumptions. However, as this model was built on the same basis of the validated above, and its results were the expected ones, it could be considered valid.

9 Evaluate the results by comparing the different technologies

As it was concluded in Chapter 8, when the variants of the SCRC were compared, intercooling in the pressurized and charger groups leads to a benefit in terms of efficiency. The same occurs when intercooling the well-known combined cycle gas turbines. This is the reason why the reference CCGT and the SCRC intercooled in both groups are contrasted in this chapter.

Both simulated plants present identical power output and a comparable fuel consumption. The fact is that the SCRC technology is supposed to use more advanced equipment than the CCGT mainly due to the larger TIT, which is around 1600 ºC. Hence, the SCRC designed reaches efficiencies about 60 %, while the CCGT designed presents a considerably lower value.

The evolution of the CCGTs efficiency from its appearance until the year 2005 is presented in Figure 9.1. The slight increase of the plant efficiency tendency during the last years might be extrapolated to future years, when the SCRC technology will be developed. Analysing the first and the second (Figure 9.2) graphics, TITs around 1650-1700 ºC will be probably reached in the future. Hence, the efficiency of the CCGT technology could approach values in the range 62-64 %.

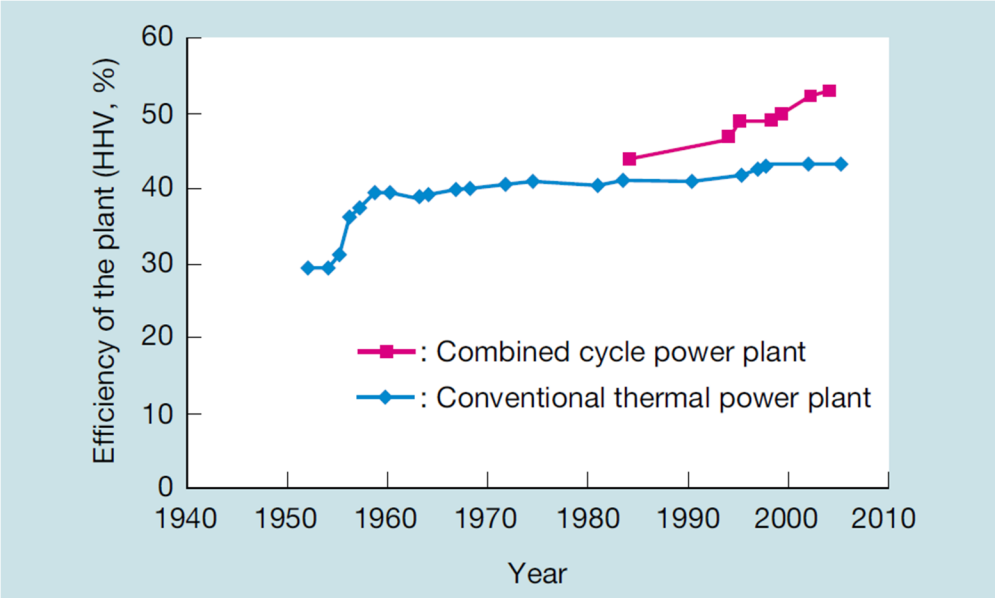

Figure 9.1 Transition of plant efficiency of conventional thermal power plant and combined cycle power plant (Ishikawa et al., 2008). The improvement in the CCGT technology leads to an increase of the efficiency.

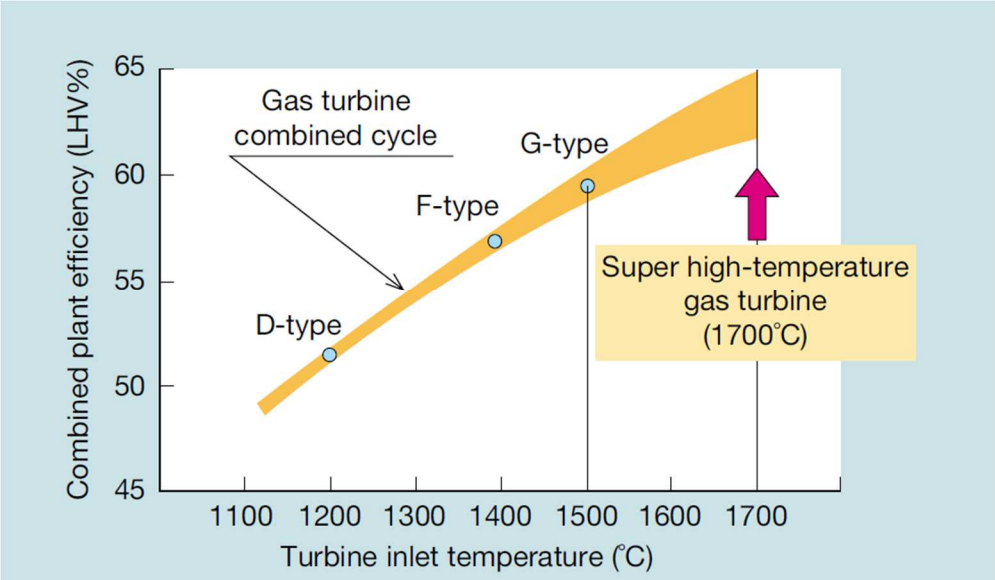

Figure 9.2 Combined plant efficiency and turbine inlet temperature (Ishikawa et al., 2008)

Being aware of this technological difference the results are presented in Table 9.1. It gives an overview of the SCRC technology compared to a current CCGT. The differences between these technologies commented afterwards will probably remain in the future.

It is worthwhile to mention that the simulation outputs match with the values shown in the theoretic Table 5.1 (Chapter 5).

Table 9.1 Comparison of the output values for the two technologies studied. Estimate numbers are indicated with an asterisk (*).

	CCGT	SCRC
Net efficiency (%)	57.7	59.6
Net power (MW)	427	427
Main compressor pressure ratio (total)	20.4*	8.9
Oxygen excess factor in combustor	2.41*	1.1
Methane fuel flow rate (kg/s)	15	14
Totally condensed water flow rate (kg/s)	0	23
Fuel gas compressor power (MW)	0	2
Combustor thermal power (MW)	971*	716
Main (gas) turbine inlet temperature	1363.9*	1595.8
Hot gas density at main turbine inlet (kg/m³)	4.3*	9.9
Main gas turbine exit flow rate (kg/s)	702	791
Main (gas) turbine average exit temperature	585.0	997.9
Flue gas stack temperature/ discharge turbine average exit temperature	79.8	185.1
Hot end temperature difference in the HRSG/recuperator	25.0	8.0
Cold end temperature difference in the HRSG/recuperator	50.7	4.3
Heat exchange in HRSG/recuperator related to power output (%)	92.4	166.6
Heat exchange in condenser/after-cooler related to power output (%)	59.3	35.7
Specific power related to the air inlet flow rate (kJ/kg)	622	1605
Specific CO_2 flow rate in discharge related to the power output (kg/kWh)	0.344	0.332

Specific power

The SCRC offers a high specific power compared to the CCGT technology. The specific power related to the air inlet flow rate reaches around 620 kJ/kg in the CCGT simulated, which is considerably lower than the specific power of the SCRC with around 1600 kJ/kg. This means that in a SCRC the inlet and outlet ducts can be built remarkably smaller.

Heat exchange requirement

The large heat exchanged requirement of the HRSG/recuperator related to the power output is interpreted as a bigger size of the HRSG compared to the heat exchange area of the condenser/after-cooler.

The heat requirement in the recuperator represents the 166.6 % of the power output, while in the HRSG it is around 92 %. However, the heat exchange in the CCGT occurs at ambient pressure compared to a pressure of around 6 bar in the SCRC case. The heat transfer coefficient increases at high pressures. Hence, the recuperator's size of the SCRC will be smaller than the HRSG in the CCGT studied. The mentioned deduction is also applicable to the condenser of a CCGT and the after-cooler of a SCRC. Therefore, the SCRC has a considerably lower footprint than the CCGT because of the higher power density of the equipment.

Pinch temperature point

Another relevant discrepancy between the HRSG of the CCGT and the recuperator of the SCRC is noticed by comparing the TQ diagrams displayed. In the SCRC two temperature pinch points occur at the hot and cold end of the recuperator while the temperature difference within the recuperator remains higher. However, in the CCGT, the two pinch points appear after heating up the steam in the superheaters. In CCGT technology the situation of these pinch points depend strongly on the pressures at which the steam is produced.

Condensed water

The SCRC technology is relevant in arid environments. While the CCGT lose all the water produced by combustion through the stack, the SCRC produces condensed water. It is for this reason that if a cooling technology is applied, the plant can still export water. For instance this water could be used for cleaning tasks.

Flue gas composition

As it can be appreciated in Table 9.2, the CO_2 and O_2 mole contents in gases out of the stack of the SCRC represents respectively 10.1 % and 1.3 % of the exhaust gas, while these fractions are 3.8 % and 12.4 % by mole in the CCGT technology. On the one hand, the SCRC is well suited for CO_2 capture because of the near stoichiometric composition and the high temperature of the gases out of the stack. Therefore, the SCRC technology pollute less than a CCGT, which directly discharges the CO_2 produced into the atmosphere. On the other hand, the low content of O_2 in the recirculated fluid of the SCRC can cause corrosion in some machinery of the cycle, and resistant materials should be used.

Table 9.2 Molar fractions of the exhaust flow out of the stack

Molar fraction (mole %)	CCGT	SCRC
Argon (Ar)	0.89	0.97
Nitrogen (N_2)	74.51	80.85
Oxygen (O_2)	12.42	1.34
Water (H_2O)	8.43	6.70
Carbon dioxide (CO_2)	3.75	10.14

Other

The high pressures and temperatures in the main machinery of the SCRC leads to use resistant materials in these devices. As it was seen in theory, the mitigation of the high pressure of the casings is to arrange the high pressure parts in a common pressure vessel. Therefore, this vessel avoid the need for a heat resistant design or insulation. This probably results in an increase of the cost of the SCRC.

Finally, an advantage of the CCGT is the fact that its behavior in direct is well known, whereas the big scale of a SCRC have still to make the step from theory to practice.

Table 9.3 summarizes all the advantages and inconveniences of the SCRC compared to the CCGT. As a conclusion, SCRC plants are a good option if the objective of the plant is to reduce emissions at the same time that a high efficiency is needed.

Table 9.3 Advantages and inconveniences of the SCRC technology

Advantages	Disadvantages
High efficiency	Use of resistant materials in some devices
Reduced size and weight of the machinery	Low O_2 content in the recirculated gas
Pinch points situated at the hot and cold ends	Possible corrosion
High CO_2 content in discharge at high temperature	Expensive
Low emissions	Not proved practically
Useful in arid conditions	Limitation in TIT
Water production	Pressure and temperature limitations
No extra bottoming cycle fluid	Fuel compressor needed
High specific power	
Smaller pipes in intake discharge points	
Low footprint	
High power density	

10 Sensitivity analysis

As it was concluded in Chapter 8, the semi-closed recuperated cycle with intercooling in all compressors is the variant most interesting to implement. A sensitivity analysis of this variant is carried out with the aim of knowing how this plant would respond to particular changes.

The method followed for doing the sensitivity analysis is to make small variations in one variable fixed during the modelling process, while the other characteristics are upkeep constant as in the base case. The results of these variations are used to comprehend how they influence the power output and efficiency of the plant.

As the model was designed, the cooling fluid temperature was fixed at 550 ºC. This temperature depends strongly on the design of the recuperator and the point where the fluid is discharged. When modelling, the temperature desired of the cooling fluid was reached by choosing the hot end temperature difference in recuperator (difference between temperatures of streams 10 and 6 in Figure 6.4), and the cooling recirculation rate (fixed at 7 % in the base case). It is for this reason that during the sensitivity analysis it is necessary to approximate this temperature to 550 ºC by changing the temperature difference mentioned above. The error derived of this procedure is negligible, and only affects some hundredths in efficiency, power output, and temperatures.

10.1 Influence of the recirculation ratio

Recirculation ratio changes have a strong influence on the efficiency of the cycle. Figure 10.1 affirms that the efficiency is roughly inversely proportional to the recirculation ratio. The power output shows the same tendency (see Figure 10.2). This is due to the increasing or decreasing of the turbine inlet temperature.

When augmenting the quantity of recirculated fluid, the TIT is increased because there is more amount of fluid to heat up. As it can be appreciated in Figure 10.3, recirculation ratios higher than 67.5 correspond to a TITs above 1600 ºC. Nowadays, there are not so many gas turbines operating that can support so high temperatures.

For all these reasons, regulating this temperature and the power output of the plant can be done by changing the rate of the recirculation ratio. If the highest efficiency possible is the aim of the plant, a lower recirculation ratios that led to reasonable TITs should be chosen.

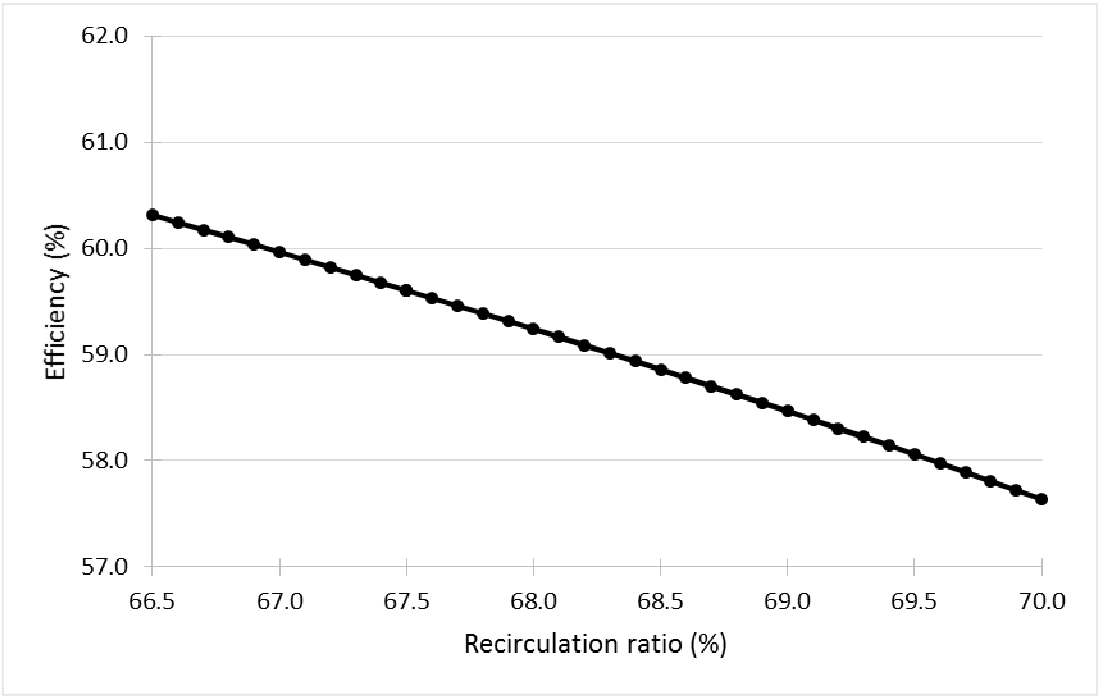

Figure 10.1 Efficiency – recirculation ratio graphic of the SCRC. Higher efficiencies are reached with low values of pressure ratios.

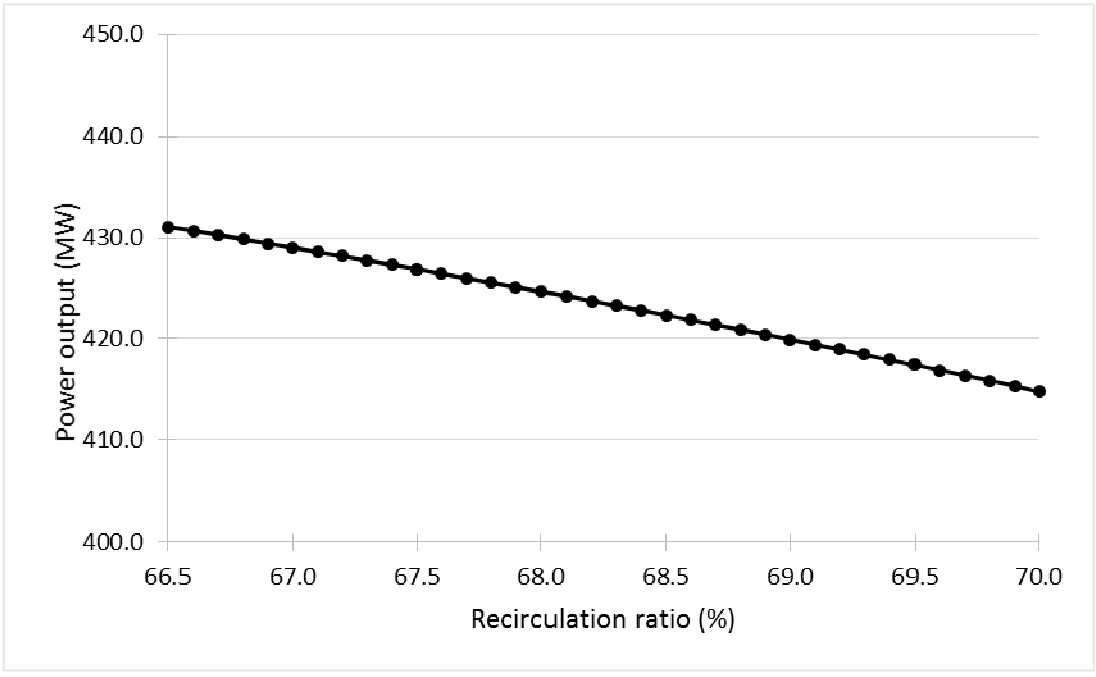

Figure 10.2 Power output – recirculation ratio graphic for the SCRC. The power output can be regulated by changing the recirculation ratio.

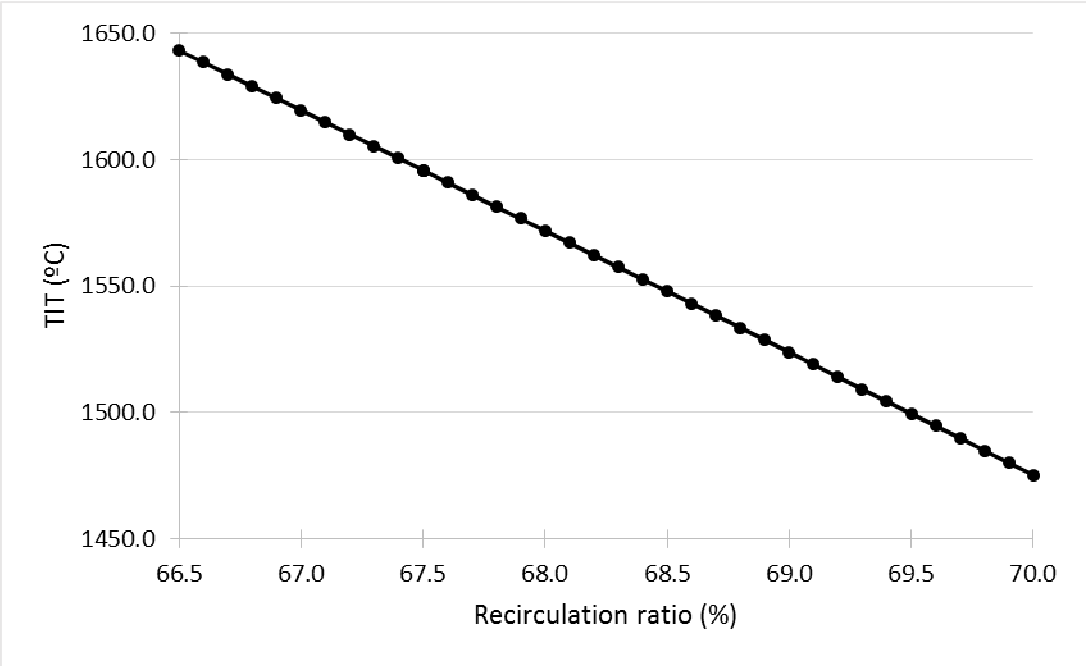

Figure 10.3 Turbine inlet temperature – recirculation ratio graphic of the SCRC. The hot gas temperature at the main turbine can be increased by reducing the recirculating ratio, and vice-versa.

10.2 Influence of pressure ratios

The effect of changes in pressure ratios of the main and charger group is relevant because it is an easy way to change the operation of the plant.

The results of variances of the pressure ratio of the main compressor are shown in Figure 10.4 and Figure 10.5. As it can be appreciated, the pressure ratio of the main loop has a large influence on the power output and efficiency of the cycle. Efficiency and power output decrease, roughly in proportion to the compressor pressure ratio. This is due to the main turbine inlet temperature diminution.

If the turbine inlet temperature would not be also affected by this change, it might be concluded that a small pressure ratio is always profitable. Nevertheless, the TIT increases when the pressure ratio decreases. In this case, for pressure ratios lower than 9.8 the TIT is above 1600 ºC. As it was commented before, it is difficult and costly to use gas turbines that can support these temperatures. An easy way to reduce this TIT could be increasing the cooling fluid ratio, or discharging the flue gas from the recuperator at higher temperature, but the efficiency would be reduced in both cases. Choosing the lower pressure ratio that allows a reasonable TIT could be the best solution if it is not desired to modify the recuperator's design.

The power output could be regulated by changing the pressure ratio of the main group, but taking into consideration how the efficiency of the cycle would affect.

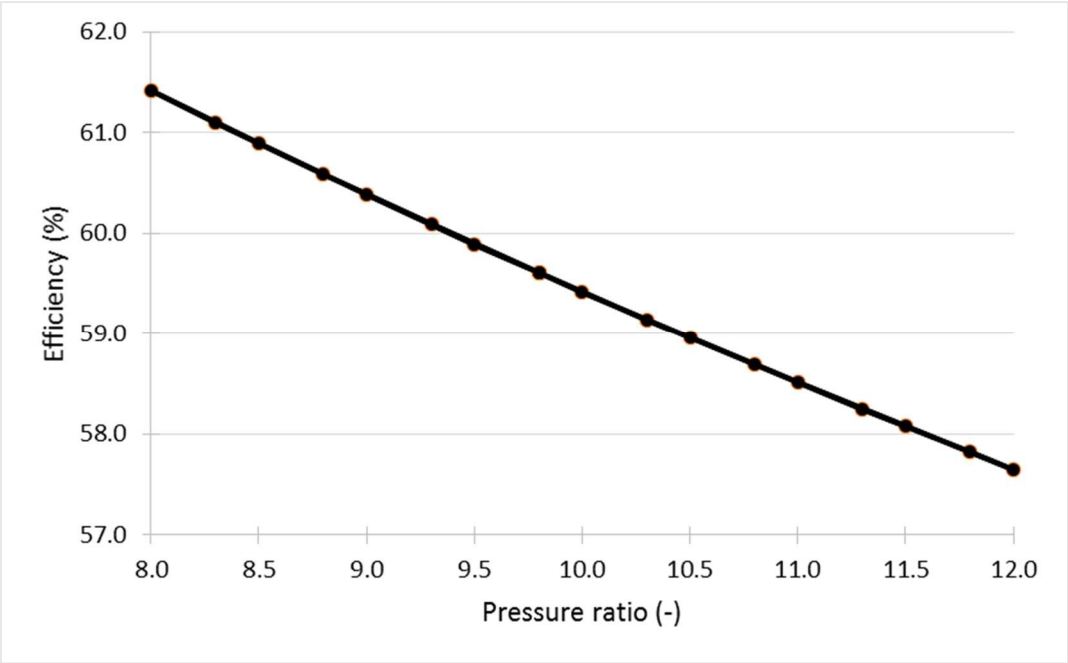

Figure 10.4 Efficiency – pressure ratio of HP loop graphic of the SCRC. The efficiency decreases if the pressure ratio increases, and vice-versa.

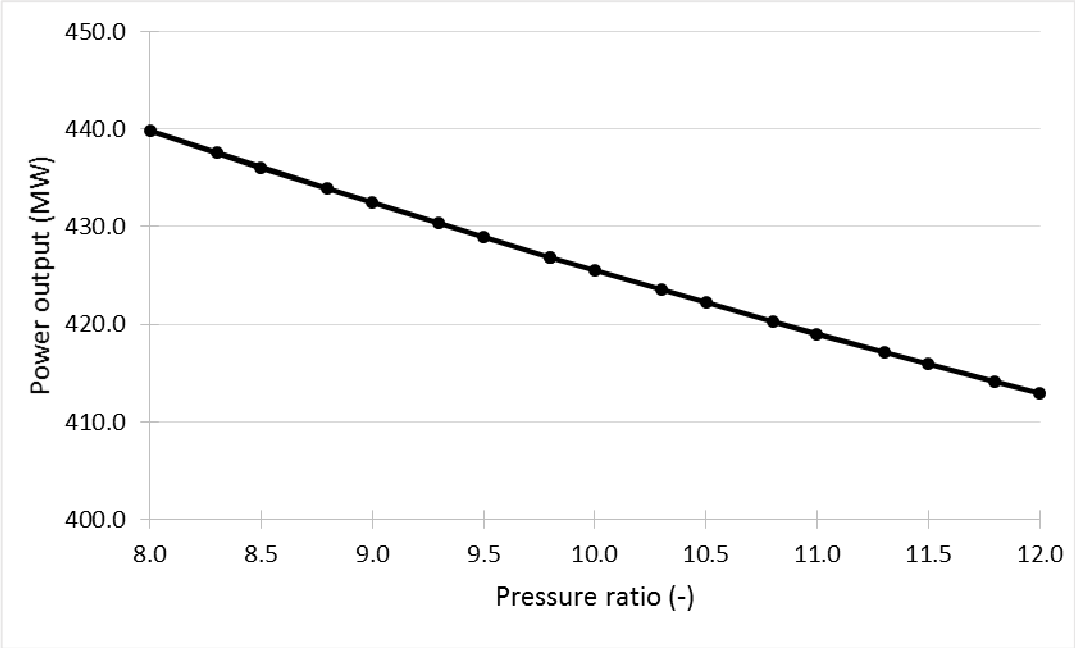

Figure 10.5 Power output – pressure ratio of HP loop graphic of the SCRC. The power output decreases if the pressure ratio increases, and vice-versa.

Besides, if the pressure ratio changed corresponds to the compressor of the charger group, the response of the plant is totally different. The efficiency remains practically constant with low-pressure ratio variances, as Figure 10.6 shows. The pressure ratio variations are in the range of

3.2-7.0. The largest value is chosen because higher ratios than 7.0 led to TITs quite higher than 1600 ºC. On the other hand, for lower ratios than 3.2, the fuel compressor is not necessary anymore (the pressure of the fuel deliberated is equal or higher than the pressure required in combustor).

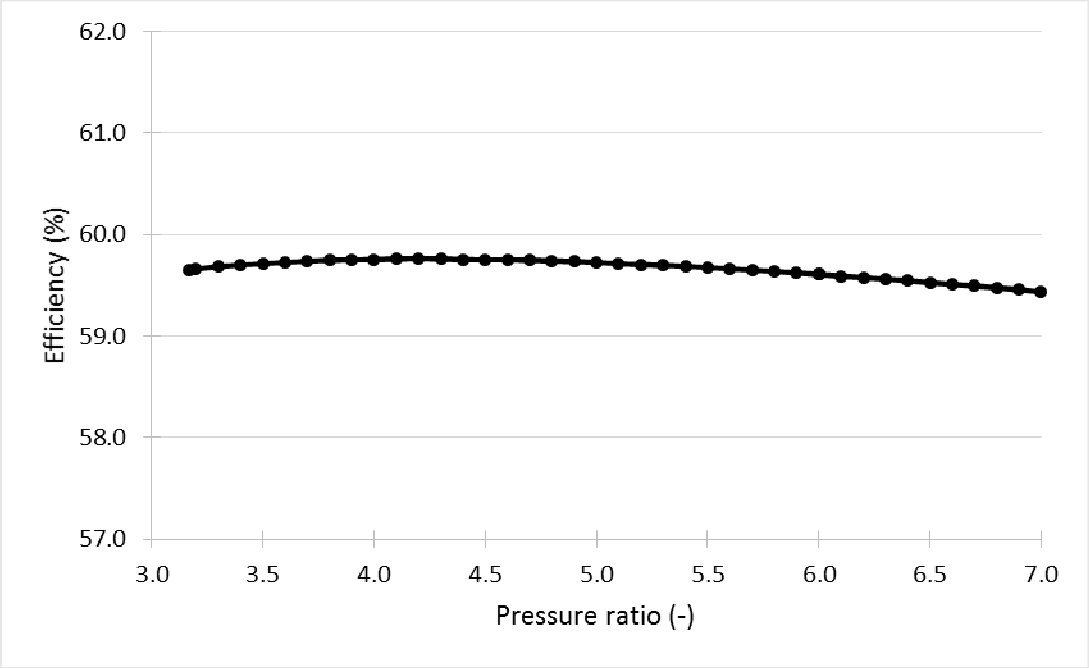

Figure 10.6 Efficiency – pressure ratio of LP loop graphic of the SCRC. The efficiency remains almost constant with the pressure ratio.

Practically, this means that the power output could be regulated by changing the pressure ratio of the charger compressor maintaining the efficiency. If losses in the mixing point had been considered, the efficiency would be diminished because of the differences between temperatures of the mixed gases. However, this reduction in efficiency might be not very significant since the mass flow introduced in the HP loop is considerably small compared to the flow recirculated.

Another propriety of the cycle is that it could be depressurized easily by changing this pressure ratio. This is important in case that the charger compressor would not work due to technical problems or a maintenance stop, because the plant could continue working and producing energy.

10.3 Influence of the cooling water temperature

Fluctuations in the cooling water temperature can be interpreted as alterations in ambient conditions. In our model, changes in cooling water temperatures are directly related to the temperature after intercoolers/after-cooler. This temperature was considered 5 ºC higher than the cooling water temperature. In the base case, the temperatures fixed were 15 ºC for the cooling water, and 20 ºC for exit temperatures of intercoolers and after-cooler.

In the following graphics are represented the cooling water temperature influence on the cycle efficiency and power output.

A diminution of the cooling water temperature enhances the power output of the plant, because the charger compressor has to work less. Therefore, the efficiency is increased some decimals and it is possible to reach efficiencies around 60 %. Quantitatively, a reduction of the cooling water temperature from 15 to 8 ºC, increases the thermal efficiency to 60.1 %, and the power output to 430 MW.

Moreover, increasing the cooling water temperature leads to a marginal increase of the TIT.

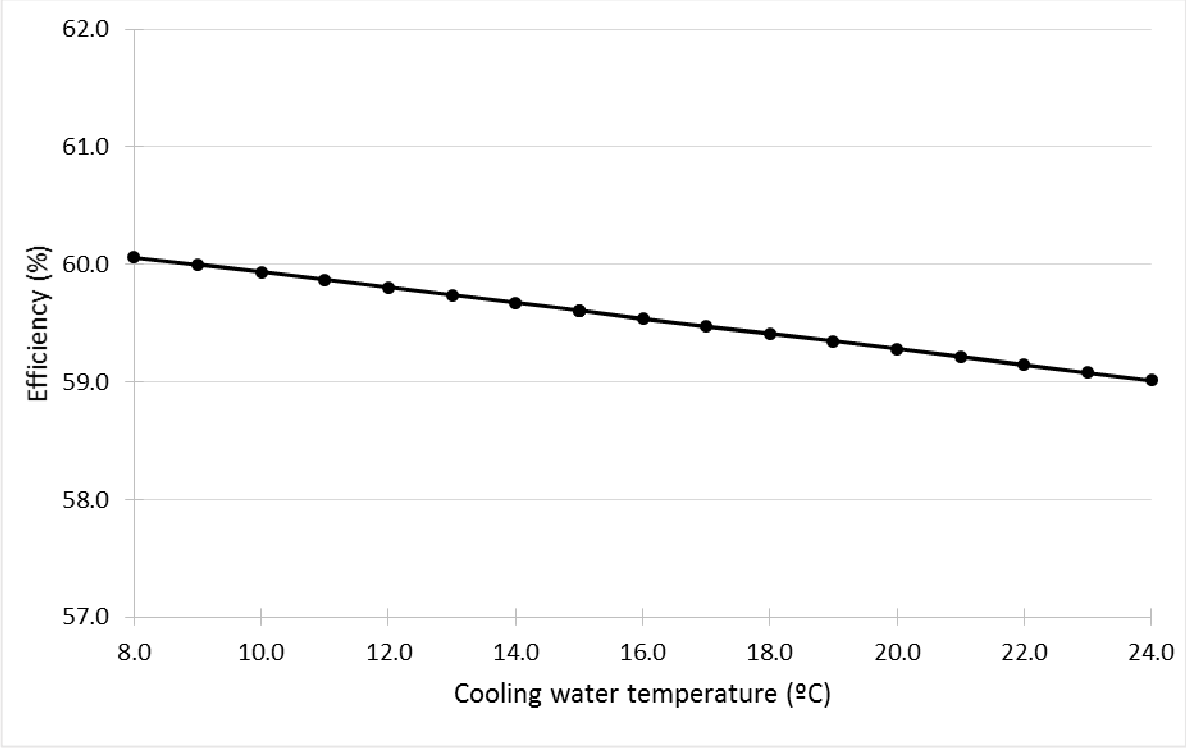

Figure 10.7 Efficiency – cooling water temperature graphic of the SCRC. A cooling water temperature diminution benefits the SCRC efficiency, as it occurs in CCGT.

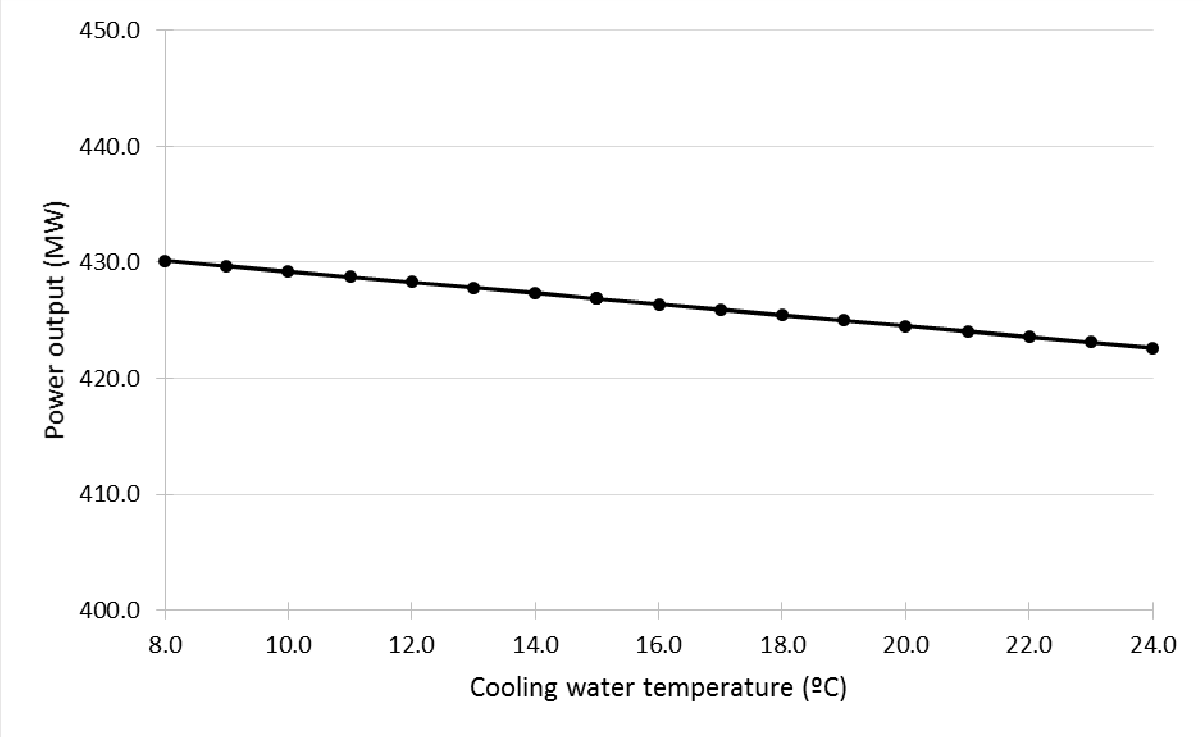

Figure 10.8 Power output – cooling water temperature graphic of the SCRC. If the cooling water decreases its temperature, the power output is slightly higher.

After interpreting the meaning of these graphics, it could be concluded that these plants would offer better results if ambient conditions are cooler. It would be preferable to situate these plants in cold places.

10.4 Influence of turbomachinery's efficiency

The influence of turbomachinery's efficiencies on the plant efficiency gives useful information about which efficiency could reach the plant if the turbines and compressors used are more advanced or not compared to the ones of the base case.

For carrying out the sensitivity analysis, the same delta (±0.1 %) is applied in all turbomachinery. The results are displayed in Figure 10.9.

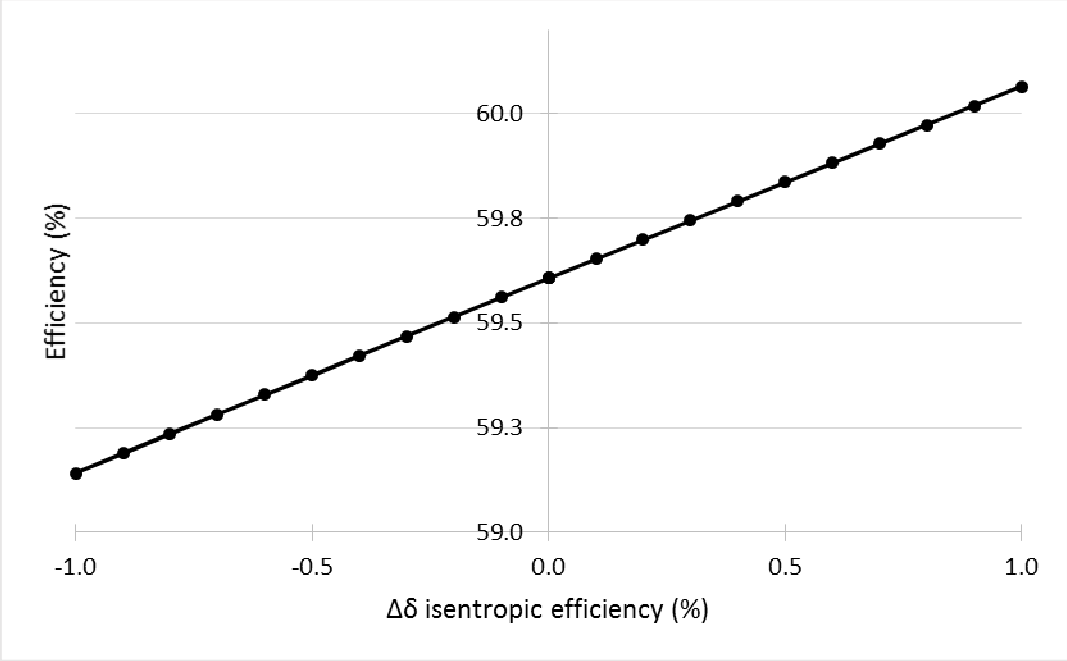

Figure 10.9 Efficiency - Δδ isentropic efficiency of the turbomachinery graphic of SCRC. If the turbomachinery technology is improved, an efficiency around 61 % could be reached.

As it is expected, an increase in the turbomachinery's efficiency has a positive effect on the plant efficiency. By reducing 1 %-point the isentropic efficiencies considered in all compressors and turbines, the efficiency of the plant is reduced, but it still keeps high (nearly 59.1 %). In contrast, if turbomachinery is improved 1 %-point, efficiencies around 61 % are achieved.

Therefore, it could be concluded that a progress in turbomachinery is beneficial for this cycle, allowing efficiencies above 60 %.

10.5 Conclusion

After making the sensitive analysis, it could be stated that the SCRC studied offers flexibility, and the capacity of adapting to different energy demands.

As it has been seen, this technology offers more than one way to control the power output, being the most useful by changing the pressure ratios. As a consequence of this, this technology could be used as a base load plant, but also could cover the demand during peak hours.

Another important characteristic is that the main loop can be depressurized easily maintaining the efficiency almost constant. In case of a maintenance stoppage in the charger group, or one of the LP compressors is broken, the plant could still produce electricity.

There are some factors that influence on the plant. Modifications of water temperatures have an important effect on the efficiency and power output. A cold environment benefits the plant, and situating it in a cold place would be advantageous. The highest efficiency would be reached during cold seasons.

Finally, the plant efficiency could be considerably enhanced if turbomachinery characteristics are improved. It has been seen that efficiencies superior to 60 % could be reached with technology improvement. This technology improvement includes a rise in turbine inlet temperatures, and therefore turbine efficiency.

This sensitivity analysis might be used for subsequent cycle optimizations. The best option might be to choose ratios which allow realistic maximum pressures and TITs.

The results of this analysis would be applicable for plants with identical (or at least close) design conditions.

11 Challenges with the SCRC technology, potential and future work

Two variants of a semi-closed recuperated cycle for electrical energy generation in onshore applications were investigated in this thesis: one intercooling only in the pressurized group, and another one which intercooled the charger and the main compressors. As it happens in combined cycle gas turbines, it was corroborated that intercooling benefits the SCRC regarding efficiency.

A detailed comparison was made theoretically and afterwards practically by simulating both cycles with EBSILON®Professional. It is worth mentioning the probably low accuracy of the outputs displayed by the software.

Regarding the comparison between cycles, the fact that the plants simulated were not at the same level technologically because the TIT was considered higher in the SCRC should be taken into account. And as it occurs in the CCGT, a higher TIT benefits this technology. A further increase in TITs represents also a challenge in SCRC.

The assumptions in the model could lead to imprecise results. Firstly, the gas circulating through the main group was considered a real gas instead of the ideal mixtures assumed in other studies. This was done because of the high pressures and temperatures reached in the SCRC. This assumption might need to be revised. Another conflicting point in the results obtained was the fact that the limitation around 900 ºC at the recuperator in the SCRC was not accomplished.

However, as the outputs obtained match with the theory and other similar studies, they might be used in future work as illustrative results. They confirm the potential of the SCRC technology when operational flexibility, efficiency and low emissions have a relevant interest.

Another contribution of this thesis is the sensitivity analysis, which contemplated the influence on the cycle of variations in recirculation ratio, pressure ratios, cooling water temperature and isentropic efficiencies of the turbomachinery. For instance, it demonstrated that a 1 %-point improvement of the efficiencies of the turbomachinery results in an increase around 2.3 % of the plant net efficiency. The influence of other variables on the cycle might be explored. One of the most interesting variable is the **increase/decrease of the fuel preheat temperature**.

During the analysis of the SCRC, a maximum pressure and main TIT were not considered. Hence, and as it was commented before, the range of some variables explored for knowing how they influenced the cycle (especially pressure ratios) did not accomplish these limitations. This

is the reason why interpreting the results of the sensitivity analysis in a general way, and taking into account the current technology limitations might be useful for **optimising** the cycle.

A simulation considering NO_x as a product of the combustion would have given more realistic results. Moreover, in this simulation the fuel was pure methane. The advantages/inconveniences of **using another fuel type/quality** might be interesting to study. The capacity to adapt a plant to different fuels allows it to continue producing energy when the typical fuel used is not available, and to negotiate fuel prices. Depending upon the fuel used and its quality, this technology could be applied to different applications.

In this thesis the SCRC was applied for onshore cases. The oil and gas companies have singular requirements for offshore installations, which in many ways are different to onshore plants. For instance, offshore plants are limited of weight and space, and therefore a high power/weight ratio is of importance. It is also required a high production, efficiency and reliability. The low power density, high efficiencies and high power between other characteristics that offers the SCRC technology might cover offshore requisites. Thus, the potential of applying this technology in **offshore plants** might be explored.

As it was concluded after the simulation results, the SCRCs could work in arid places due to its capacity to produce condensed water under ISO conditions. Therefore, a **design using dry cooling systems** might be of interest.

Renewable sources have a relevant paper in the future because the other energy sources are scarce. From an operational viewpoint, the integration of renewables constitutes a significant challenge due to the stochastic property of most of the renewable sources. The production variability of these technologies – specifically wind power plants (see Figure 11.1) – have to be compensated by non-stochastic power plants. Currently this function is carried out by CCGTs, but it is very costly due to the continuous changes in production levels, and to the fact that they have to start up and shut down often (Gil et al., 2014).

It is necessary a technology flexible enough in the short term to provide backup in the face of variability and uncertainty. Guaranteeing supply in the medium term by securing adequate amounts of primary energy is also needed.

And the SCRC technology might be a better alternative than the CCGTs to handle the so-called power cycling. This is the reason why a study of the SCRC plants in this situation might be relevant. For achieving this, first **off-design simulations**, and lately **transient/dynamic simulations** might be explored.

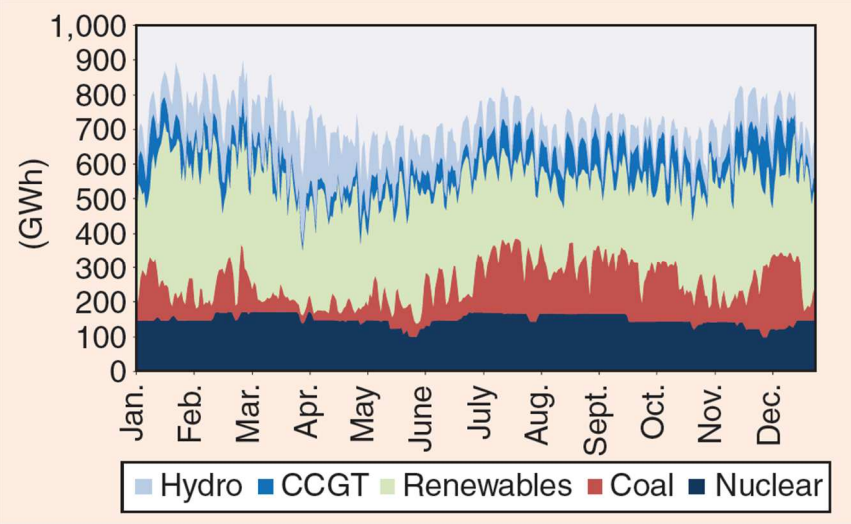

Figure 11.1 Electricity production in Spain by source of primary energy (Gil et al., 2014). It can be appreciated the high variability production of renewables sources, and the consequent adaptation of the CCGTs to these changes.

Apart from the importance of the renewable sources, low emissions are in the spotlight. In order to reduce carbon emissions, one option is the **CO_2 capture**. The flue gas contains a high CO_2 concentration and the required low temperature heat extraction for driving a CO_2 absorption (Wettstein, 2013). The absorption process of the CO_2 contained in the discharged gas of the SCRC was not considered as part of this current work, and might be further investigated.

There are still open issues that might be explored before launching this product. Regarding the devices' design of a SCRC plant, the high-pressure level and temperatures might be a design challenge. A detailed study of arranging the pressurized part in one vessel might be further investigated in its mechanical and thermal aspects.

The design of the recuperator is another conflictive point of this technology due to the high pressures and temperatures at which it works. In the theoretical part of the thesis, the existence of a pressurized direct contact steam generator was found. The characteristics at which this device works match with the gas that flows through a recuperator of a SCRC (low O_2 content, high CO_2, and high pressures). The idea of applying a similar technology in the recuperator of the SCRC might be explored.

A study of a **safety operation and maintenance** of the semi-closed cycle is another open issue. It would be an interesting study due to the high pressures in the cycle, and especially when handling fuel gas under high pressure.

Finally, the creation of a first **small unit size** would be interesting for demonstrating that this technology can make the step from theory to practice. To carry this out it would be necessary to first study more conservative designs. To change from small to big scale, an **economic** study might be done. This study could include the best optimization of the cycle taking into account the equilibrium between costs of the plant and a high efficiency.

12 Conclusion

Full-plant simulations of two variants of the novelty semi-closed recuperated cycle, the intercooled variant comparison to a common combined cycle power plant, and a sensitivity analysis of determined variables for this variant are presented herein. The design of the cycles were applied to onshore cases. Thus, the results and the comparison of both cycles were discussed taking into account the basic needs of an onshore plant.

This comparison showed that the SCRC technology is able to reach high efficiencies and power output at probably the same level than an advanced CCGT plant. The advantages compared to the CCGT technology are mainly four:

1. Its capacity of production water under ISO conditions.
2. Its simplicity and the avoidance of a bottoming cycle fluid.
3. The reduced size of the machinery and therefore its lower footprint.
4. Low CO_2 emissions due to the fact that the properties of the discharged fluid (high CO_2 content and temperature) make this technology suitable to use absorption methods for capturing the CO_2.

The lately sensitivity analysis of the SCRC model demonstrated the capacity of this plant to control the power output by different ways, which can be translated as an inherent property of flexibility. As it occurs in CCGTs, it was seen that changes in the cooling water temperature have a high influence on the plant's efficiency. Finally, it was concluded that the plant efficiency could be considerably enhanced if turbomachinery characteristics are improved.

To summarize, the SCRCs could outperformance in different aspects the CCGTs and could be of relevant importance in a period that clean sources are of vital importance. SCRC technology offers a flexibility that could face future energy demands while offering high efficiencies and low emissions if the CO_2 is captured.

Its low power density leads to think that this technology might be applicable in other cases such as in offshore plants. There are still lines of investigation that might be explored before launching this technology, but its potential is clear.

13 References

ANSALDO ENERGIA. *AE94.3A Gas Turbine brochure* [Online]. Available: http://www.ansaldoenergia.it/easyUp/file/gas_turbine_ae94_3a_english_jun2014_pdf.pdf [Accessed 27 January 2015].

ANSALDO ENERGIA. *Power generation solutions* [Online]. Available: http://www.ansaldoenergia.com/easyUp/file/pgs.pdf [Accessed 27 January 2015].

BOLLAND, O. 2009. Thermal Power Generation. *Compendium.* Department of Energy and Process Engineering NTNU.

BOLLAND, O. & SÆTHER, S. 1992. New concepts for natural gas fired power plants which simplify the recovery of carbon dioxide. *Energy Conversion and Management,* 33**,** 467-475.

CAIRNS, P. E. 2013. *High Pressure Oxy-fired (HiPrOx) Direct Contact Steam Generation (DCSG) for Steam Assisted Gravity Drainage (SAGD) Application.* University of Ottawa.

CANADA'S OIL SANDS INNOVATION ALLIANCE. 2015. *Direct Contact Steam Generation* [Online]. Available: http://www.cosia.ca/initiatives/water/water-projects/direct-contact-steam-generation [Accessed 13 March 2015].

CLEMENTS, B. 2009. High Pressure Direct Contact Oxy-Fired Steam Generator. Google Patents.

ENGE, Y. O., WIRSUM, M. & WETTSTEIN, H. E. 2006. The Potential of Recuperated Semiclosed CO2 Cycles. *ASME Turbo Expo 2006: Power for Land, Sea, and Air*. Barcelona, Spain: American Society of Mechanical Engineers.

FRUTSCHI, H. U. 2005. *Method for operating a partially closed, turbocharged gas turbine cycle, and gas turbine system for carrying out the method.*

GIL, J., CABALLERO, A. & CONEJO, A. J. 2014. Power Cycling: CCGTs: The Critical Link Between the Electricity and Natural Gas Markets. *Power and Energy Magazine, IEEE,* 12**,** 40-48.

GUETHE, F., STANKOVIC, D., GENIN, F., SYED, K. & WINKLER, D. Flue gas recirculation of the Alstom sequential gas turbine combustor tested at high pressure. ASME 2011 Turbo Expo: Turbine Technical Conference and Exposition, 2011. American Society of Mechanical Engineers, 399-408.

INTERNATIONAL ENERGY AGENCY 2012. *World Energy Outlook 2012*, Paris, France, OECD Publishing.

ISHIKAWA, M., TERAUCHI, M., KOMORI, T. & YASURAOKA, J. 2008. Development of high efficiency gas turbine combined cycle power plant. *Mitsubishi Heavy Industries, Ltd. Technical Review Vol. 45 No,* 1.

KEHLHOFER, R., RUKES, B., HANNEMANN, F. & STIRNIMANN, F. 2009. Combined-Cycle Gas and Steam Turbine Power Plants. 3rd ed. Tulsa, Oklahoma: PennWell.

LIEUWEN, T. C. & YANG, V. 2013. Gas Turbine Emissions. New York, United States of America: Cambridge University Press.

LLYWODRAETH CYMRU WELSH GOVERNMENT 2014. Implementing the Emissions Performance Standard: Further Interpretation and Monitoring and Enforcement Arrangements in England and Wales. *In:* CHANGE, E. C. (ed.). London.

MORAN, M. J. & SHAPIRO, H. N. 2006. *Fundamentals of Engineering Thermodynamics*, Hoboken, New Jersey, Wiley.

RAO, A. D. 2012. Combined Cycle Systems for Near-Zero Emission Power Generation. Woodhead Publishing.

STEAG ENERGY SERVICES GMBH. *EBSILON®Professional for engineering and designing energy and power plant systems* [Online]. Available: www.ebsilon.com [Accessed 16 January 2015].

UNITED STATES ENVIRONMENTAL PROTECTION AGENCY. 2014. *Standards of Performance for Greenhouse Gas Emissions From New Stationary Sources: Electric Utility Generating Units* [Online]. Federal Register. Available: http://www.gpo.gov/fdsys/pkg/FR-2014-01-08/pdf/2013-28668.pdf [Accessed 27 January 2015].

WETTSTEIN, H., WIRSUM, M. & SCHULZ, S. 2010. Gasturbinenanlage mit abgasrückführung sowie verfahren zum betrieb einer solchen anlage. Google Patents.

WETTSTEIN, H. E. 2013. Air Breathing Semi-closed Recuperated Cycle and its Super Chargeable Predecessors. *Gas Turbine World 2013,* 42.

WETTSTEIN, H. E. SCRC Technology for Naval Propulsion. ASME 2014 12th Biennial Conference on Engineering Systems Design and Analysis, 2014a. American Society of Mechanical Engineers, V002T09A002-V002T09A002.

WETTSTEIN, H. E. 2014b. The Semi-Closed Recuperated Cycle with Intercooled Compressors. *ASME Turbo Expo 2014: Turbine Technical Conference and Exposition.* Düsseldorf, Germany: American Society of Mechanical Engineers.

ZWEBEK, A. & PILIDIS, P. 2003. Degradation Effects on Combined Cycle Power Plant Performance—Part I: Gas Turbine Cycle Component Degradation Effects. *Journal of Engineering for Gas Turbines and Power,* 125**,** 651-657.

Appendix

Table 0.1 Stream table of the first variant (SCRC). Numbering in accordance with Figure 6.3 in Chapter 6.

Stream nr	P (bar)	T (ºC)	m (kg/s)	Composition (mole %)					
				Ar	N_2	O_2	CO_2	H_2O	H_2O (l)
1	5.897	20.0	778	1.00	83.376	8.164	7.068	0.397	0.000
2	18.576	141.1	778	1.00	83.376	8.164	7.068	0.397	0.000
3	18.019	20.0	778	1.00	83.376	8.164	7.068	0.129	0.003
4	18.019	20.0	777	1.00	83.600	8.185	7.087	0.130	0.000
5	57.792	143.4	777	1.00	83.600	8.185	7.087	0.130	0.000
6	54.950	993.6	722	1.00	83.600	8.185	7.087	0.130	0.000
7	52.752	1664.9	737	0.96	80.652	0.846	10.362	7.176	0.000
8	55.881	550.0	54	1.00	83.600	8.185	7.087	0.130	0.000
9	52.752	1595.8	791	0.97	80.852	1.343	10.140	6.699	0.000
10	6.266	997.9	791	0.97	80.852	1.343	10.140	6.699	0.000
11	6.141	411.5	257	0.97	80.852	1.343	10.140	6.699	0.000
12	1.014	185.1	257	0.97	80.852	1.343	10.140	6.699	0.000
13	1.013	15.0	266	0.92	77.393	20.646	0.026	1.010	0.000
14	6.079	227.7	266	0.92	77.393	20.646	0.026	1.010	0.000
15	6.079	151.4	534	0.97	80.852	1.343	10.140	6.990	0.000
16	6.079	176.2	800	0.95	79.694	7.803	6.756	4.795	0.000
17	5.897	20.0	800	0.95	79.694	7.803	6.756	0.379	0.044

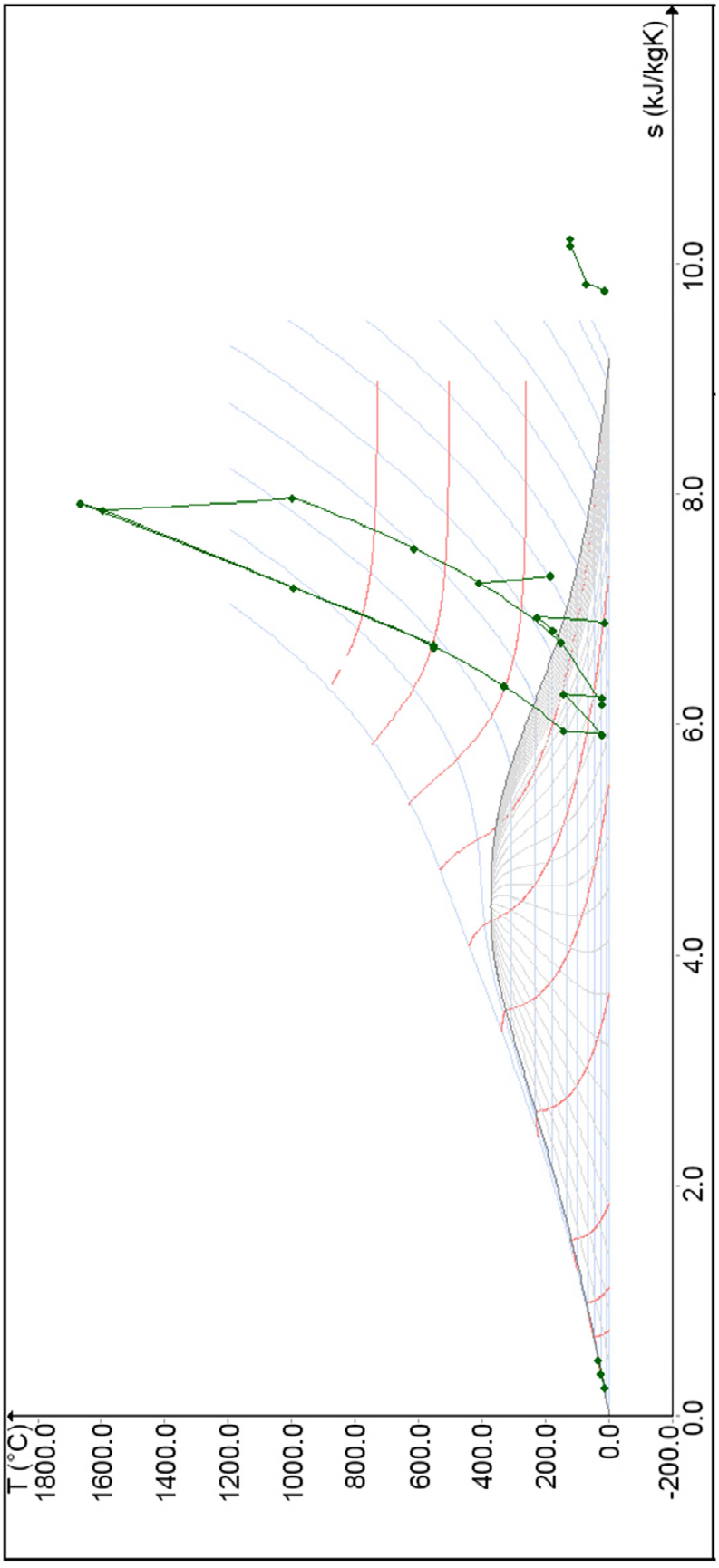

Figure 0.1 Temperature – specific entropy diagram of the first variant (SCRC)

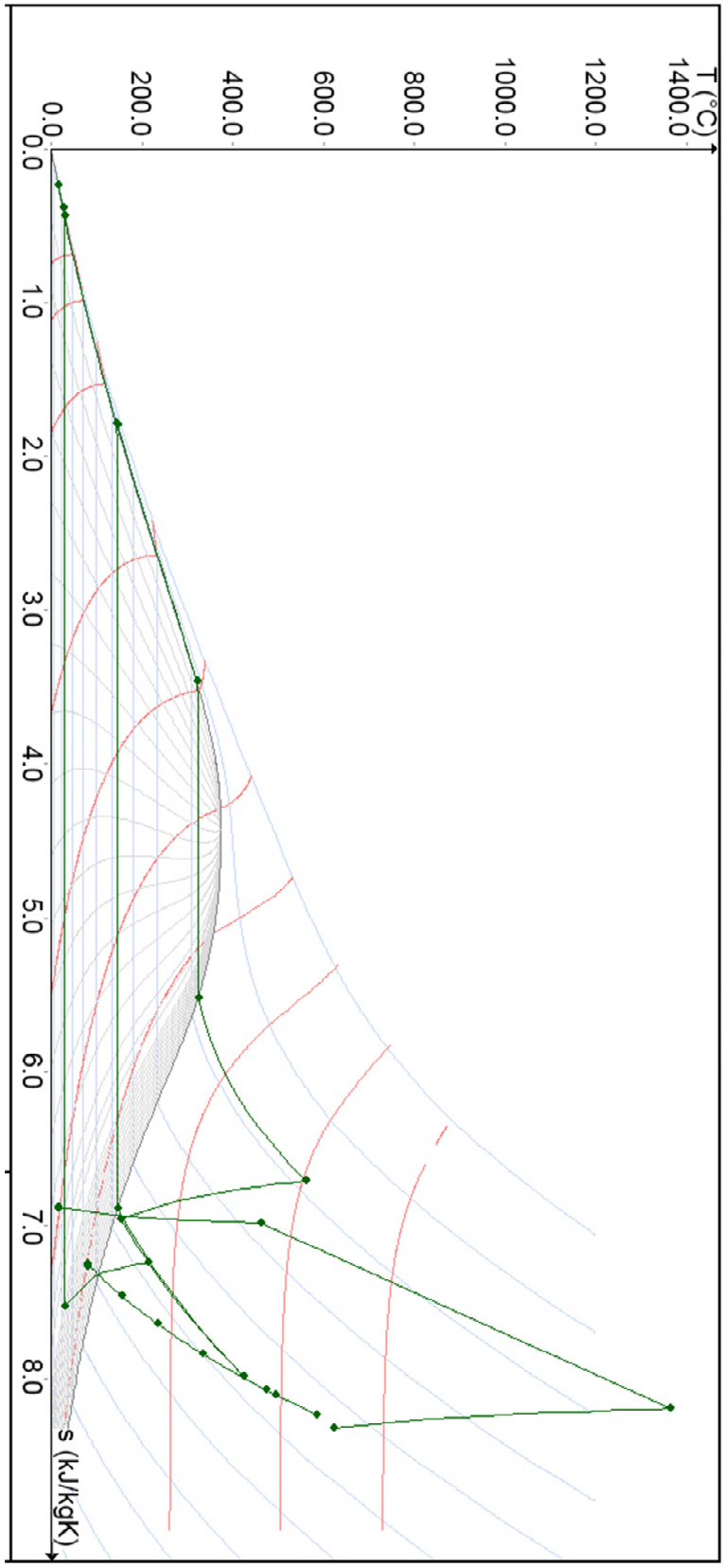

Figure 0.2 Complete temperature – specific entropy diagram for the combined cycle gas turbine designed (GT cycle approximated)